Selected Articles on
TIME DOMAIN REFLECTOMETRY
Applications

HEWLETT **hp** PACKARD

APPLICATION NOTE 75

SELECTED ARTICLES ON TIME DOMAIN REFLECTOMETRY APPLICATIONS

TABLE OF CONTENTS

TIME DOMAIN REFLECTOMETRY
THEORY AND APPLICATIONS

by
Lee R. Moffitt

Hewlett-Packard Company
Colorado Springs Division
Colorado Springs, Colorado

Time-Domain Reflectometry– Theory and Applications

LEE R. MOFFITT, Hewlett-Packard Co., Colorado Springs, Colo.

Time-domain reflectometry (TDR) is a measurement concept that is beginning to find great usefulness in the analysis and synthesis of wideband systems. The art of determining the characteristics of electrical lines by observing reflected waveforms is not new. In fact, power-transmission engineers have located discontinuities in power-transmission systems for many years by monitoring reflections from an electrical pulse.

This investigative technique is particularly useful because the amplitude of the reflected signal directly corresponds to the impedance of the discontinuity. Also, the distance to the reflecting impedance can be determined from the time the pulse takes to return. The limitation of this method is the minimum system rise time. The total rise time consists of the combined rise time of the driving pulse and that of the oscilloscope that monitors the reflections. For instance, if a transmission line is excited by a square-wave generator with a 20-nsec rise time and the reflections are monitored with a 50-Mc oscilloscope, the resulting rise time of the system is about 21 nsec. A fast rise time allows identification of discontinuities that are close together. The distance to a discontinuity is given by $d = ct_0/2$ where c is the speed of light and t_0 is the elapsed time between generated and reflected pulses. The distance between two discontinuities is

$$d = \frac{c(t_1 - t_2)}{2}.$$ It becomes impossible to distinguish between pulses when $t_1 - t_2$ is half of the system rise time t_r. Thus, the minimum distinguishable distance between pulses is $d = ct_r/4$ and a 21-nsec rise time will give 1.57-meter resolution.

In resolving reflections, the technique used is analogous to any form of scanning. For instance, in a television vidicon tube, the faster the rise time of the scanner, the greater is its ability to resolve detail in the subject scanned.

The recent advent of sampling oscilloscopes with effective response beyond 4 Gc, and the development of subnanosecond solid-state switching devices, have made it possible to extend the reflectometry method to give a resolution of less than 1/2 inch. For example, if a generator has a 50-psec rise time and an oscilloscope has 100-psec rise time, the resolution becomes

$$d = \frac{(3 \times 10^8 \text{m/sec})(\sqrt{25 + 100} \times 10^{-11}\text{sec})}{4}$$

$$= 0.84 \text{ cm.}$$

TDR BASICS

The TDR analysis begins with the propagation of a step or impulse of energy into a system and the subsequent observation, also at the point of insertion, of the energy reflected by the system. Several arrangements are possible, but the following procedure is used by the newer specialized reflectometers. A fast step is developed in a generator that is matched to a 50-ohm line. The incident step passes through a feed-through sampler and is sent into a coax cable that is attached to the circuit element or antenna being tested. The oscilloscope is attached to the feed-through sampler and the incident step, along with the reflected waveform, is displayed on its face. By analyzing the magnitude, duration and shape of the reflected waveform, the nature of the impedance variation in the transmission system can be determined.

Resistive Loads

If a pure resistive load is placed on the output of the reflectometer and a step signal is applied, a step signal is observed on the CRT whose height is a function of the resistance(Fig. 1). It is a good practice to separate the system under test from the TDR unit by at least 8 inches of 50-ohm cable. This moves the reflections away from the leading edge of the step, such that overshoot and ringing are not superimposed on the observed signal. The magnitude of the step caused by the resistive load may be expressed as a fraction of the input signal as given by $\rho = \dfrac{R_L - 50}{R_L + 50}$.

Reactive Loads

For reactive loads, the observed waveform depends upon the time constant formed by the load and the 50-ohm source (Fig. 2).
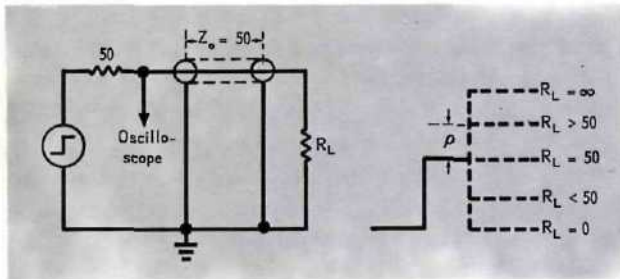
Consider the case of a coaxial cable terminated in a resistive load. Because of the lead length in the load, there is excess inductance. By use of TDR (Fig. 3) we can determine quite simply:

   a. The characteristic impedance of the cable
   b. The degree of resistive mismatch in the termination
   c. The amount of excess inductance in the termination
   d. The length of the cable

TDR IN PRACTICE

Time-domain reflectometry has many advantages over conventional CW reflectometry. Discontinuities in a system are clearly separated *in time* on the CRT. Therefore, it is easy to see the mismatch caused by a connector, even in the presence of a bad discontinuity somewhere else in the system. It is even possible to determine which connector is

FIG. 1 — *Step signal-height variations resulting from different resistive loads.*
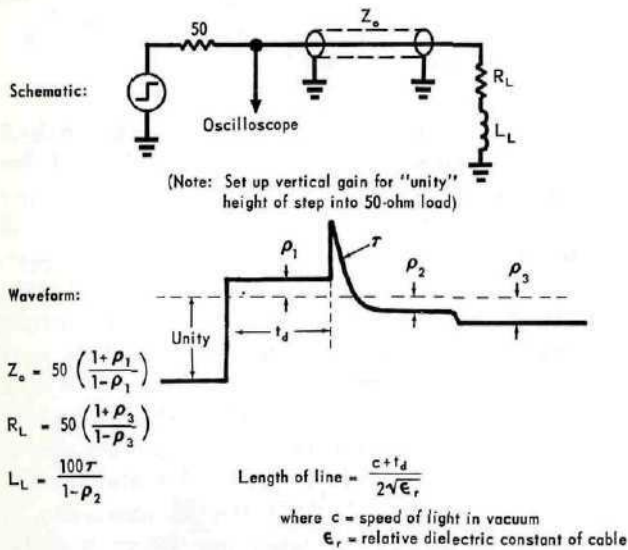
FIG. 2 — *Both resistive and reactive impedances can be calculated readily from TDR waveshapes.*
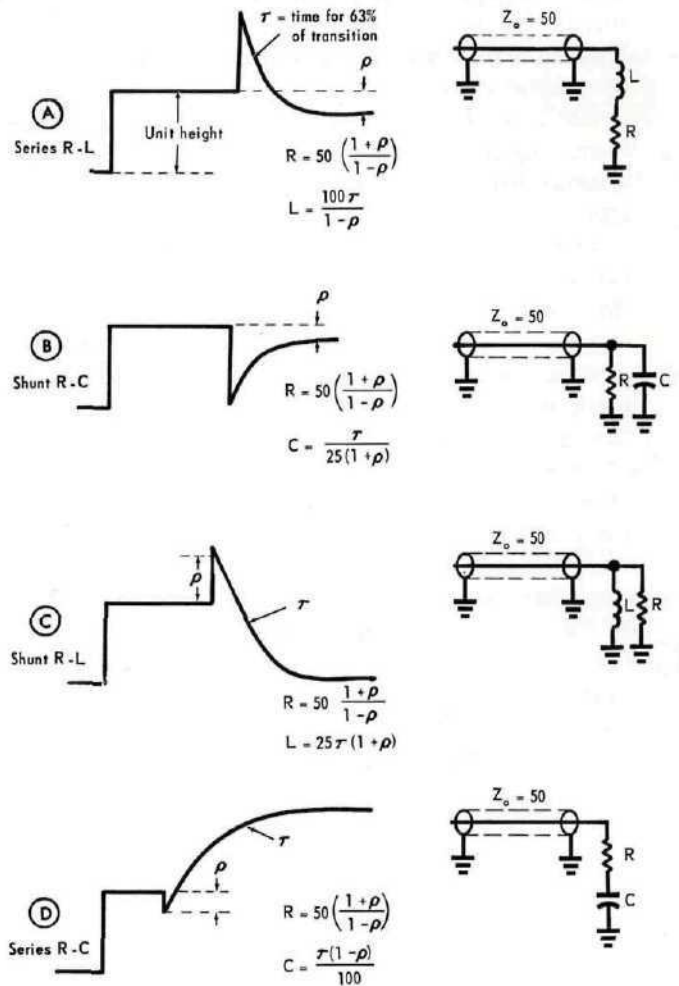

FIG. 3 — *Complete line and load characteristics can be determined easily from TDR waveshape.*

troublesome and in what way. Having determined that a discontinuity appears in a waveform, it is simple to locate it in the system, using the equation

$$d = \frac{ct}{2\sqrt{\epsilon_r}}$$

where ϵ_r is the relative dielectric constant of the transmission system. A timesaving procedure is to calibrate the system such that 1 cm on the horizontal axis is the equivalent of the certain number of centimeters for the coaxial line. Again the limiting factor is the system rise time. Thus, any discontinuities spaced closer than

$$d = \frac{c\, t_r}{4\sqrt{\epsilon_r}}$$

will appear as a single discontinuity.

The finite rise time also places a lower limit on the size of the reactive impedance than can be distinguished. For example, a small shunt capacity in a 50-ohm system will cause the waveform to depart from the ideal response (Fig. 4). The height of the actual response, normalized to the step height, is given by

$$\alpha = \frac{MCZ_o}{2}$$

in the case of a capacitor, or $\alpha = ML/2Z_o$ for an inductor, where M is the maximum slope of the normalized incident step, measured at the point of discontinuity. As an example of the nonideal response, if M is 1.3×10^{10} then α's of 2×10^{-3} can be observed. These are realistic values well within the capability of modern TDR equipment. Equipment with these capabilities can measure capacitances down to 6.2×10^{-15} farads, or inductance to 1.5×10^{-11} henries.

The maximum observable line length is a function of the repetition rate chosen. This determines the
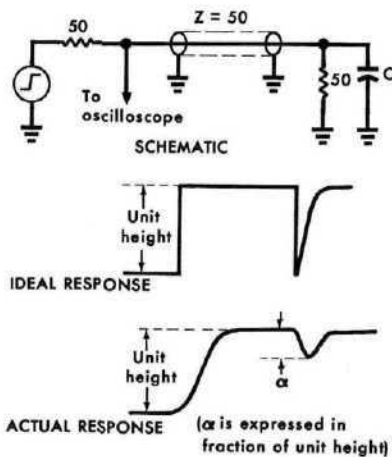

FIG. 5—*Time-domain reflectometer unit shown plugged into HP 140A sampling oscilloscope.*
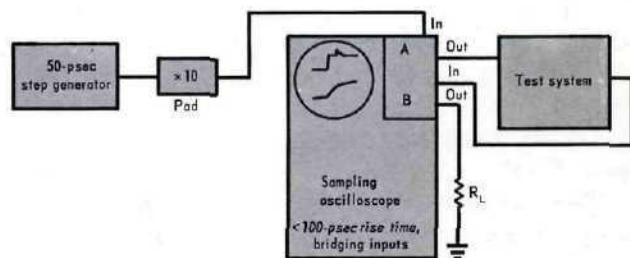

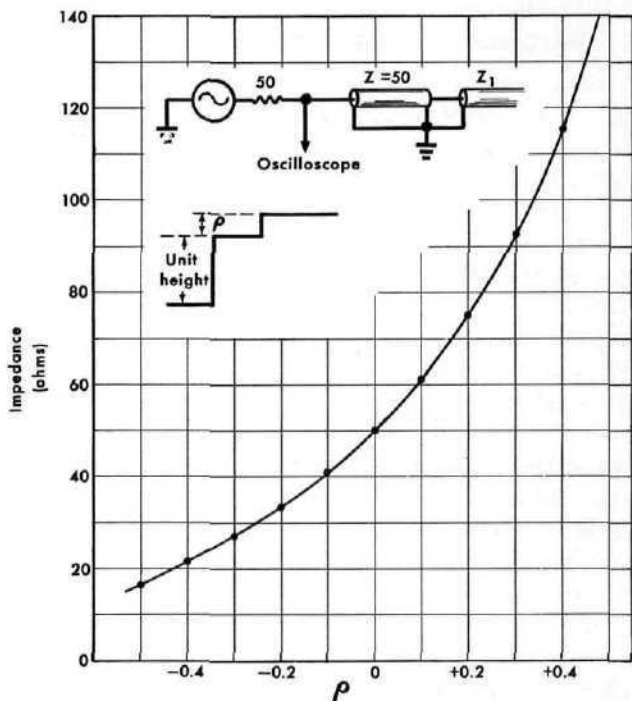FIG. 6—*Dual-channel oscilloscope allows analyzing of both reflection and transmission characteristics.*

FIG. 7—*Curve for the conversion of normalized reflected pulse height into system impedance.*

FIG. 4—*Small shunt capacity in system degrades ideal response.*

duration of the pulse after its rise. Since only the rising step is observed, the oscilloscope is blanked during the return step and for a period thereafter long enough to allow the falling step to propagate, reflect and be absorbed.

The upper limit on measuring reactive elements is set mainly by the inconvenience that results from the time constants being so long that successive steps overlap. If t_{max} is arbitrarily set to 0.8 μsec and the system has a repetition rate of 200 kc, then capacitances up to 0.016 μf or inductances to 0.04 mh can be measured. By observing the fractional change in the voltage waveforms per unit time, it is possible to measure much larger components. Using this technique, it is possible to extend the range of measurements to 5 μf and 12 mh.

The 200-kc repetition rate permits the use of TDR devices with up to 1000 ft of air dielectric cable or 670 ft of polyethylene dielectric coax.

RANGE AND RESOLUTION OF IMPEDANCE MEASUREMENTS

Assuming $Z_o = 50\Omega$, resistors between 0.025Ω and 100k may be measured. Because the resistance is directly a function of the step height, by using a precalculated transparent overlay, the resistance may be determined directly.

One common use of TDR is the analysis of the coaxial cable. The amount of impedance variation that can be detected in a long section of cable is a function of the flatness of the top of the incident step function. If this step is flat within ± 1/2 percent, impedance variations of 1/2 ohm along the cable can be detected, corresponding to a 1-percent check on cable impedance. Thus, irregularities in cable makeup resulting from vibrations in the braiding process or tightness of the insulating jacket show up clearly. For short sections of

cable, impedance variations of much less than 1/2 percent can be observed.

Practical Hardware

The HP Model 1415A is a unit that illustrates the attainable capabilities of a TDR. The unit contains a pulse generator, sampling channel and associated circuitry (Fig. 5).

It is often desirable to incorporate sampling circuits to provide analog signals for an X-Y recorder. Where a large number of records must be kept, for proof of performance or later comparison, X-Y records are less costly than oscilloscope photos. Their large size also makes measurement more convenient.

For applications where the output of a test system is of interest, a dual-channel sampling oscilloscope can be used in a TDR configuration to display both the input and transmission characteristics of the system (Fig. 6).

TIPS ON TDR TECHNIQUES
Preparation and Calibration

The generator is connected to the sampler channel and an accurate 50-ohm termination is connected to the output. For the initial setup, however, this termination can be a 1-percent film resistor with short lead lengths. The vertical gain is adjusted to give a 10-cm step, and the 50-ohm termination is removed and test system is connected.

The magnitude and location of reflections can be viewed more closely by choosing an appropriate time scale and verticle magnification. Calibration of the horizontal deflection allows rapid physical location of points of interest. Calibration of the vertical axis in terms of reflection coefficient allows interpretation of results directly in terms familiar to engineers who have been using the conventional VSWR measurements.

With the instrument calibrated, cable impedance can be determined from the height of the

reflected step. The graph shown in Fig. 7 may be used to translate step heights into impedance.

For balanced systems, it is convenient to use a balun transformer consisting of a length of coaxial cable wound around a ferrite toroid (Fig. 8). One unit of this configuration, the HP H10-185B matches a 200-ohm balanced system, with an output pulse that is flat within 10 percent for 2 μsec.

FIG. 8—*Balun transformer couples pulses into balanced systems.*

For a system with a large number of bad mismatches, great care must be taken to avoid confusion because of rereflections. These rereflections usually can be separated and identified by deliberately worsening each known mismatch in turn and observing the change in reflected waveform. Disturbances caused by rereflections will increase when the primary mismatches are worsened. Often the best procedure, when faced with a complex situation such as this, is to start at the input end of the test system and clean up the discontinuities successively from that end. The ability to interpret the signals physically, as in the TDR system, makes this a comparatively simple procedure.
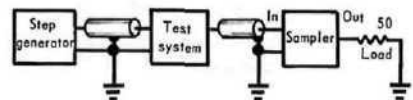

FIG. 9—*Block diagram for time-domain transmission testing.*

Auxiliary Techniques

If the purpose of the system being analyzed is primarily to transmit a signal without dis-

tortion, it may be helpful to work on the basis of time-domain transmission in addition to TDR. After the system has been optimized at the input port by reflectometry, the system is connected between the step generator and the sampler (Fig. 9). Here a terminating oscilloscope is equally useful unless the system's own load must be included in the observation. The transmitted step is observed and checked for overshoot, rise time and other criteria that may apply.

The transmitted signal may be checked at any point within the system by using a resistive divider probe that minimizes circuit loading. This is connected by a cable to the input of the sampler channel and used to trace the step through the system. This is an alternative to reflectometry that is often useful.

Analyzing Connectors And Terminations

Departures from 50 ohms in a connector or termination can cause large reflections in a pulse system, or a large VSWR in a system that carries primarily sinusoidal signals. Unfortunately, even the best connectors cause reflections or a varying VSWR because of human errors in the assembly process. Therefore, it is not sufficient to rely on buying expensive connectors to insure freedom from unwanted reflections. In this respect, TDR relieves this worry by rapidly showing where the mismatches are, how bad they are and if they are capacitive or inductive, series or shunt. Fig. 10 shows a step being propagated from a section of RG9A/U into a load. The connectors on the load and cable are the General Radio Type 874. Four different cases are shown with varying loads, thus illustrating how the connection and the load can be analyzed by using the TDR.

Cable Impedance

The most convenient method of making precise measurements of cable impedance on the reflectometer is to connect a section of air line with precisely determined impedance between the test cable and the TDR unit. The step height through the airline section sets the 50-ohm level. Variations from this level in the test cable are noted, and the cable's impedance is calculated

(Fig. 11). In this test, the impedance level of the test line is $Z_o = 50 \frac{1 + \rho}{1 - \rho}$ where ρ is the reflection coefficient of the reflected mismatch. The change in amplitude shows ρ to be +0.03, so $Z_o = 50\left(\frac{1.03}{.97}\right) = 53$ ohms.

The impedance of a long section of cable would be exactly Z_o if the cable were completely lossless. However, most cables
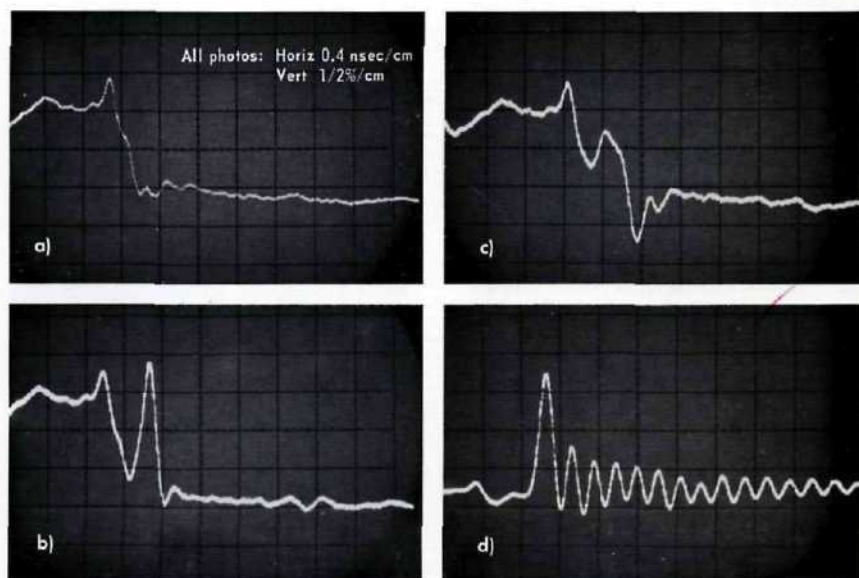

FIG. 10—*Waveforms resulting from using different loads. The loads are (a) precision high-frequency load. Positive spike indicates slight inductance in connector. Drop of 1 percent indicates 51-ohm cable. (b) High-frequency connector with 1.5-percent spike indicating 0.1-mh inductance within connector. (c) Transition from GR-N adapter (male) through N (female) back to GR874 connector and into 50-ohm load. (d) Ringing resulting from improperly mated connectors.*
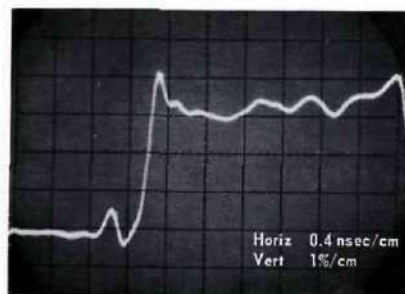

FIG. 11—*Oscillograph of step from air line into test cable.*

FIG. 12—*Trace of cable shows construction irregularities and increasing series resistance.*

have a small series loss and a negligible shunt loss. This series resistance adds to Z_o and causes the impedance level, as observed from one end of a cable, to increase as longer sections of cable are observed. The slope on the step height that results from the increasing impedance is evident in Fig. 12.

Other applications where the TDR method of analysis can be used effectively are the component characteristic analysis and antenna analysis. The components can be placed in an appropriate jig and the TDR method used to determine their shunt capacity and series inductance (Fig. 13).

In investigating antennas, the TDR pattern will not be a simple one, but instead will present a complex reactive profile (Fig. 14). Once the proper profile for a particular antenna is determined, any improper construction details can be detected and the proper corrective action determined (Fig. 15).
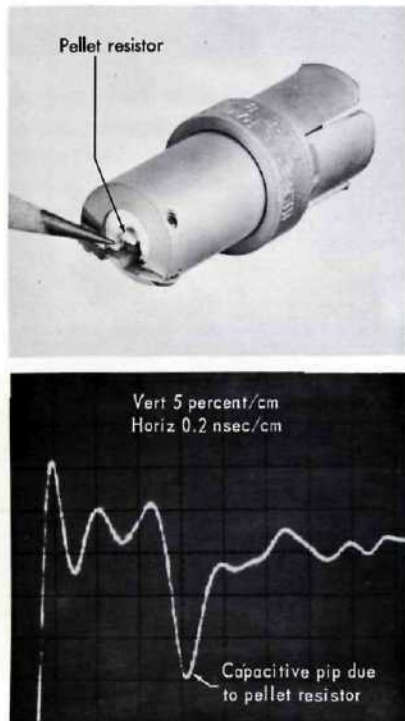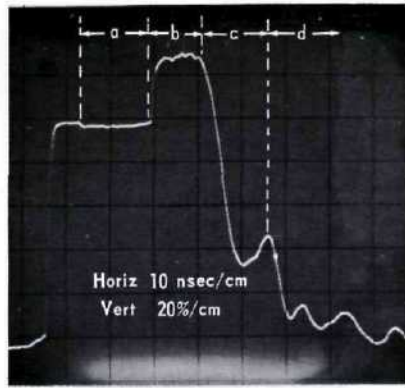

FIG. 14—*Scope trace of antenna with (a) 50-ohm feedline, (b) 75-ohm antenna, (c) short at end of antenna and (d) rereflections.*
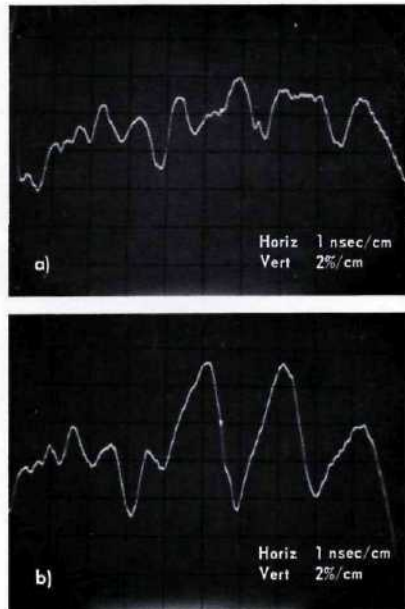

FIG. 15—*Complex reactive profile of (a) good antenna and (b) antenna that has had one of its dipoles lengthened 2 inches.*

CONCLUSION

Time-Domain Reflectometry can be a powerful tool in the design and subsequent production and analysis of wideband transmission systems. It can reveal sources of trouble and opportunities for improvement that have not been previously apparent. Used with swept Frequency-Domain Reflectometry methods, it can contribute to rapid achievement, and proof, of performance levels not previously attainable.

FIG. 13—*Pellet resistor checked for shunt capacity using special jig.*

TRANSMISSION LINE PULSE REFLECTOMETRY

by
Lawrence S. Kreyer

Edgerton, Germeshausen & Grier, Incorporated
Las Vegas, Nevada

TRANSMISSION LINE PULSE REFLECTOMETRY

Lawrence S. Kreyer

Edgerton, Germeshausen & Grier, Incorporated
Las Vegas, Nevada

SUMMARY

Pulse reflection measurement techniques are widely used in nuclear weapon diagnostics to measure coaxial transmission line electrical lengths and to examine them for gross discontinuities. The techniques for making such measurements are discussed in this report, and the impact of the sampling oscilloscope on these measurement techniques is described. A sampling scope/digital XY recorder with outputs suitable for automatic machine data processing is described, and computer plots of such data are shown.

Background

One of the recurrent problems in weapons tests at the Nevada Test Site is the laying of the coaxial cable from the detector to the recording station. In order to give as great a range of detector sensitivities as possible, very sensitive detectors must be placed up against the bomb case and coaxial cables run to the recording station. The times to be measured are very short, and the signals generated cannot be transmitted over open wires or by radio.

Further, we must know the relative time differences of our coaxial cable runs to less than a nanosecond, in order to make a meaningful alpha measurement. These cable runs are normally 3000 nanoseconds to 5000 nanoseconds and comprise of a variety of impedances and velocity constants.

Transmission Lines

Because they are comparatively easy to work with, coaxial cables are very widely used to transmit signal information between these non-adjacent locations. However, electrically they are composed of distributed elements as opposed to the lumped elements of familiar electrical circuits. They work very well for steady-state signals, or signals whose frequency components lie below a few megacycles per second. Unfortunately, by the very nature of distributed systems, coaxial cables inherently introduce distortion in nonsteady state signals with frequency components extending above a few megacycles per second. This distortion occurs because certain physical parameters of the cable are subject to frequency effects and therefore change their values as the frequency of the transmitted signal changes.

The characteristic impedance of a line is the ratio of the voltage to the current in an individual wave at any point on the line; it is also the impedance of a line that is infinitely long or the impedance of a finite length of line when the load impedance equals the characteristic impedance ($Z_L = Z_0$). To a TEM wave the characteristic impedance is a pure resistance and its value is independent of frequency.

The Z_0 of a coaxial transmission line is a function of the log of the ratio of the outside diameter of the inner conductor (d) to the inside diameter of the outer conductor (D).
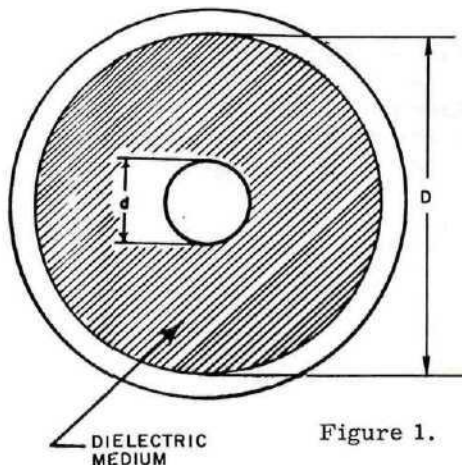

DIELECTRIC MEDIUM

Figure 1.

$$Z_0 = \sqrt{\frac{138}{\varepsilon}} \; Log_{10} \frac{D}{d}$$

ε = Dielectric Constant
= 1 in Air

It is easy to see that the line must stay concentric if the characteristic impedance is to remain the same. Any bends, dents or deviations from the dimensions dictated by the ratio between the conductors results in unwanted reflections by perturbing the symmetry of the TEM wave. These discontinuities, as they are called, do not allow a true picture of the input to be reproduced, and hinder data reduction greatly.

Reflections are generated whenever a signal traveling in a transmission line strikes a discontinuity or a gradual change in dimension (diameter of the coax line) or impedance. At the reflection point some (or all) of the incident energy is reflected back to the source and some (or none) is transmitted in the orignal direction. In most cases, reflections due to moderate changes in dimension of the line are of minor consequence. So we will consider only impedance discontinuities.
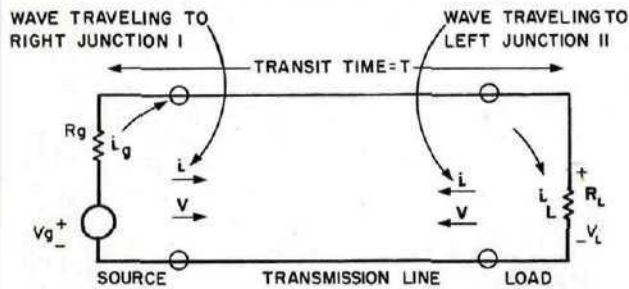

Figure 2. Transmission Line Voltage and Current Distribution Showing Traveling Waves.

Pulse Reflection Measurement

Impedance discontinuties can be located and measured most easily by applying the pulse reflection measurement technique.

The pulse reflection measurement technique is the observation of reflections along a transmission line when a step function is applied to the sending end. This observation is usually made at the sending end with an oscilloscope. The portion of incident energy which is reflected back to the sending end is added to the energy of the outgoing step. We compare the magnitude of the reflection to the magnitude of the incident pulse in order to evaluate the nature of the discontinuity. Further, we measure the time-history of the transmission line from the sending end to the receiving end. Each discontinuity is evaluated for magnitude and sign of reflected energy, and time of occurrence. This time of occurrence is related to distance along the line for trouble shooting applications, but we are mainly interested in measuring the time at which these discontinuities occur.

Pulse Generator/Oscilloscope Technique

In the past we have made these measurements by the combination of a pulse reflection measurement technique and a time interval measurement technique. The pulse reflection measurement technique consisted of conventional pulse generator/oscilloscope combination operated as described earlier. The raster oscilloscope display was used for improved time base resolution. The resolution of this display was still quite low, only location of gross discontinuities could be made to the nearest hundred feet, due to the limited band pass of this system.

Figure 3. Raster Display of Transmission Line Reflections, 100 ns Time Marks.

A second measurement was introduced in order to make accurate cable electrical length measurements. This measurement technique consisted of a lay line oscillator made up of a pulse generator and the transmission line. The frequency of this oscillator was measured on an electronic counter, as shown in the diagram below.
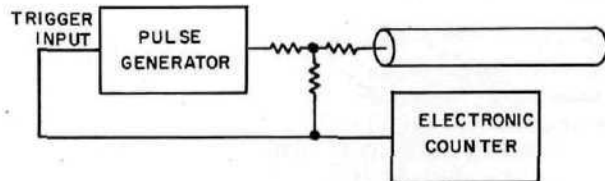

Figure 4.

The electrical length of the cable being measured is one half the reciprocal of the frequency read on the electronic counter minus the loop time of the pulse generator circuit. Measurements made using this technique are accurate to one or two nanoseconds on long cable runs, as long as gross discontinuities do not exist in the transmission line.

Sampling Oscilloscope Technique

Recently, we have been using the sampling oscilloscope to make this measurement because of its greater bandwidth and better time resolution. The sampling oscilloscope has the added advantage of a manual scan, which allows the

generator to operate low frequency recording equipment from the sampling head, thus eliminating the CRT and deflection amplifiers.

We have built one experimental system, which converts the output from the sampling oscilloscope into a format suitable for direct processing by a computer.
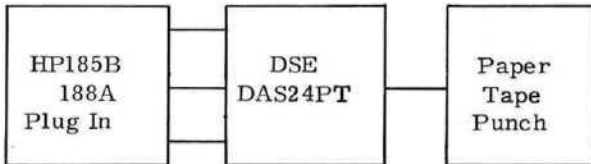

Figure 5.

This technique has important applications in the measurement of the relative electrical lengths of a large number of long transmission lines. High resolution is maintained by programming the computer to compare the rise fronts of the two pulses under study for a comparison of arrival times at 50% levels.

An example of this technique is shown in Figure 6, an XY plot of an HP 215 pulse generator output pulse.
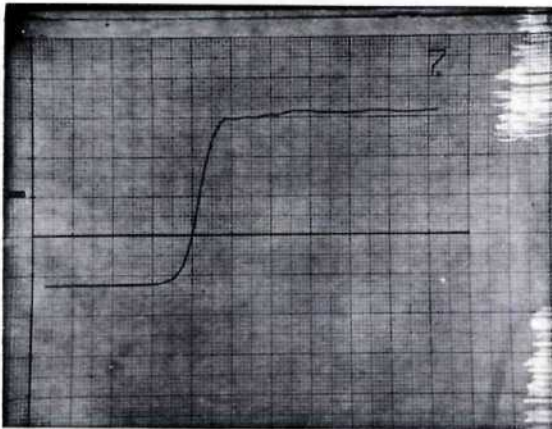

Figure 6.

This XY plot was made from a CDC 165-2 digital incremental plotter. Compare this with Figure 7, an XY plot of the same pulse taken from a analog XY plotter.
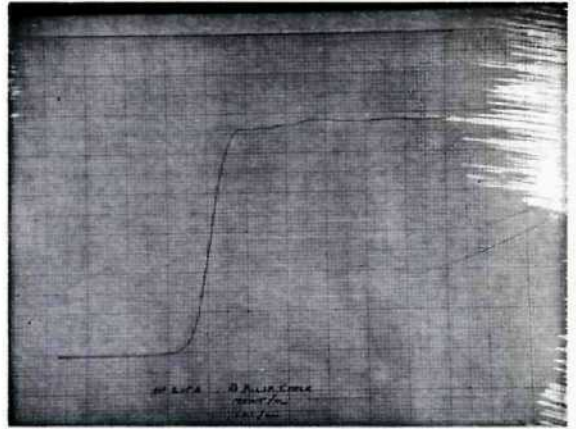

Figure 7.

Time interval measurements are made using this technique, as shown in Figure 8. The upper trace shows the signal arrival times at the A and B channels on an HP 185B sampling oscilloscope.
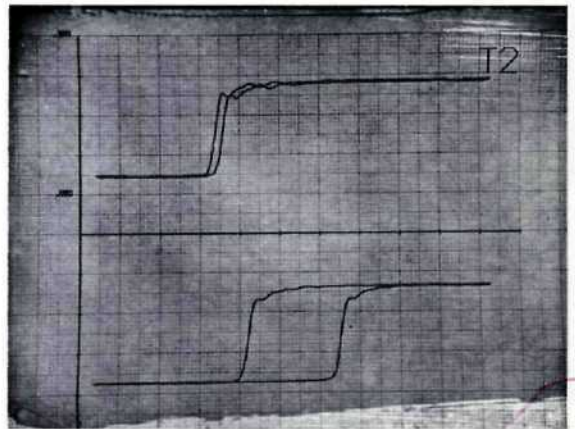

Figure 8.

System cabling prevents our having absolute simultaneous pulses at these inputs, therefore it is necessary to subtract the upper trace from the lower in order to measure the real time difference. A program has been written for the CDC 1604 computer which allows the automatic comparison of 50% levels between any two pulses, irrespective of the rise times involved. This is shown in Figures 9 and 10. Both figures are the time difference plots between 3324.6 nanosecond of 7/8" 100 ohm styroflex and 3730.9 nanosecond of 7/8" foamflex. Although the velocities of these two cables are quite different, relative time measurements can be made in the order of picoseconds by a careful analysis of their rise fronts and by the computational accuracy of the digital

computer. Figure 9 is a plot of the data prior to smoothing. On this particular test, radio frequency interference was quite pronounced at 2500 Mc.
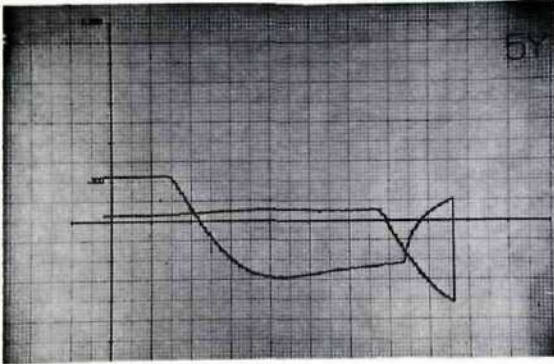

Figure 9.

The data was smoothed as shown in Figure 10 by programming a notch filter response, thus eliminating this interference.
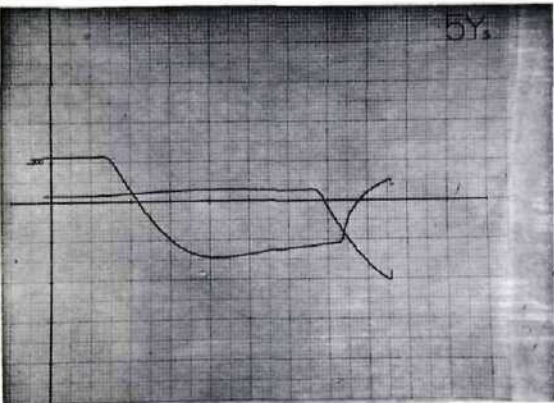

Figure 10.

CONCLUSIONS

The sampling oscilloscope has made a significant advance to pulse reflection measurement techniques. It is now possible to measure cable discontinuities which were masked by the low resolution of other instruments. Time difference measurements can be made on transmission lines to at least an order of magnitude better precision, because of the resolution of the sampling scope/ XY recorder system and the computational accuracy of the digital computer.

ACKNOWLEDGEMENTS

It is a pleasure to acknowledge the support of Mr. J.W. Sedlmeyer, Mr. R.D. Hansen, and Mr. R.D. Stoessner, who aided greatly in the setups and measurement techniques.

REFERENCES

1. "Time Domain Reflectometry", Application Note 62/Hewlett Packard Company.

2. "Cable Testing With Time Domain Reflectrometry", Application Note 67/Hewlett Packard Company.

3. "An Improved Cable Length Measurement Technique", L.S. Kreyer, EG&G Interoffice Memorandum, 19 January 1965.

4. "Digital Cable Length Measuring System", R.D. Hansen, EG&G Technical Memorandum, L-44.

5. "EG&G Procedures Manual for LASL Alpha Systems", EG&G Technical Memorandum, L-103.

6. Skilling, H.H., "Electric Transmission Lines", McGraw Hill Book Co., 1951.

7. Operation and Maintenance Manual Model DAS24PT Data Acquisition System, Dynamic Systems Electronics Company.

MECHANICAL SCALING ENHANCES TIME DOMAIN REFLECTOMETRY USE

by
Howard Poulter

Hewlett-Packard Company
Microwave Division
Palo Alto, California

With Permission of Author
Presented at WESCON 1965

MECHANICAL SCALING ENHANCES TIME DOMAIN REFLECTOMETRY USE

Howard Poulter
Hewlett-Packard Company
1501 Page Mill Road, Palo Alto, California

SUMMARY

Time Domain Reflectometry (TDR) is a relatively new tool for the microwave engineer. As with any new measurement technique it takes time to learn how to use it effectively. This paper reviews briefly the assumed capabilities of TDR today. In addition, it shows how the designer can use mechanical scaling in conjunction with TDR to extend the effective measurement frequency.

INTRODUCTION

Advantages of TDR

Time Domain Reflectometry, referred to as TDR from here on, is still a new tool for the microwave engineer. Even so, it has already earned the reputation of a "best buy" in test equipment. With further emphasis on precision coaxial connectors to 18 GHz its importance will continue to grow.

TDR has the advantage of being able to display impedance discontinuities with time substituted for distance. Thus, TDR performance is not limited by connector performance, slotted line residual or slope, or directional coupler directivity. The bad connector will be separated in time from the small reflection one wishes to observe.

Apparent Limitations of TDR

The predominant limitation to date has been assumed to be in microwave measurements above 2 GHz. Another limitation has been the ability to resolve closely spaced discontinuities. This relates to frequency range, also, because two equal discontinuities of opposite sign spaced one inch apart have essentially no net reflection at 500 mHz. However, at 3 GHz the reflections will add on a VSWR measurement. With TDR they will not be visible.

As with most good tools, a little ingenuity on the users part can overcome the apparent limitations. The rest of this paper will be devoted to that end.

THE MEASUREMENT SYSTEM

The following discussion is built around the performance of the 1415 TDR plug-in for the hp 140 scope. This is the most readily available, easily usable piece of test equipment especially designed for this purpose. Increased performance can be obtained at substantially higher cost and measurement system complexity. The important performance parameters are a system rise time of 150 picoseconds and a maximum calibrated sensitivity of 5 millivolts per centimeter. The step generator puts out a step of 1 volt amplitude and 50 picoseconds rise time.

CURRENT MEASUREMENT CAPABILITIES

Reactive Measurement Capabilities

The principal measurement limitation has been in the measurement of small shunt capacities or series inductances. It is just such elements that cause the greatest trouble in microwave device matching. Assuming one centimeter deflection, this system can measure elements as small as 100 picohenries or 0.04 picofarad.[1,2] This corresponds to a VSWR of 1.025 at 2 GHz.

As indicated earlier there is increased interest in coaxial devices up to 18 GHz. To make measurements to VSWR's = 1.01 reactive at 18 GHz requires at least twenty times increase in performance.

There does not appear to be any practical limitation on the measurement of small resistive changes except for the one of spacing. With a one millivolt sensitivity one can measure resistance changes of 0.1 ohms. Contrast this to the best alternative readily available, a 40 db directivity coupler. Such a coupler has an ambiguity of 1 ohm at an arbitrary phase angle in a 50 ohm system.

Resolution of Closely Spaced Discontinuities

The other high frequency limitation is the ability to resolve two closely spaced discontinuities.[1,2] With the present system to completely resolve two discontinuities they must be separated by the velocity of propogation in the medium times the rise time. For air dielectric this corresponds to 4.5 centimeters. Figure 1 illustrates the response of two equal capacitive discontinuities spaced 5, 2.5, and 1.0 centimeters apart in air line. The inked trace is the system rise time.
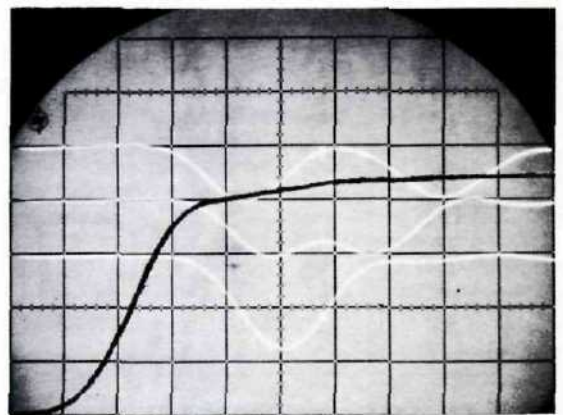

Figure 1.   Resolution of Two Discontinuities

MECHANICAL SCALING EFFECTS

Effect on Characteristic Impedance

What happens to characteristic impedance in TEM lossless systems when one scales all dimensions

by the same factor? It is almost second nature to a microwave engineer that impedance is unchanged by a scaling of all dimensions. However, consider the equation

$$Z_o = \sqrt{\frac{L}{C}} \qquad (1)$$

L = Inductance per unit length
C = Capacitance per unit length

Consider a one centimeter length of line with inductance L and capacitance C. Now double all dimensions including length. The energy stored in the electric and magnetic fields is given by

$$\text{ELECTRIC ENERGY STORED} = \int \frac{\epsilon E^2}{VOL^2} dVOL \qquad (2)$$

$$\text{MAGNETIC ENERGY STORED} = \int \frac{\mu H^2}{VOL^2} dVOL \qquad (3)$$

Now electric energy storage is directly related to capacitance and magnetic energy storage to inductance. Since all dimensions are doubled the total volume is increased by 8. However, the spacing between inner and outer conductors is only doubled so that the electric field E is reduced to one half. Since electric energy storage is related to E^2 times volume, the total electric energy and hence the capacitance varies linearly with the scaling factor. By a similar reasoning the inductance also varies linearly with dimensional scaling.

Since characteristic impedance varies as the ratio of L to C it remains unchanged by a scaling of all dimensions.

Effect on Discontinuity Capacitance and Inductance

What is the effect of scaling of dimensions on discontinuity inductance or capacitance? At a change in the transverse dimensions in a coaxial structure higher order waves are excited.[3, 4] As above, the electric fields will be decreased by the scaling factor. However, the volume occupied by these fields goes as the scaling factor cubed. As before, using equation (2), the total discontinuity capacitance is increased by the scaling factor.

COMBINING MECHANICAL SCALING WITH TDR

Derivation of Scaling Factor

From the foregoing the advantages of mechanical scaling become readily apparent. The most important is that one can build a larger model and thus scale up the discontinuity capacitance until it becomes measurable. The scaling also separates successive discontinuities in distance. This increases our effective resolution by the same scaling factor.

How does one determine the necessary scaling factor? Assume that one has a coaxial device that one wants to match up to frequency F_1. Assume that the maximum reflection that can be allowed is ρ_1.

As mentioned earlier, the minimum capacitance one can measure with the 1415 is

$$C_{MIN} = 0.04 \text{ picofarad} \qquad (4)$$

The reflection from a small reactive shunt discontinuity is given by

$$\rho = \frac{Z_L - Z_o}{Z_L + Z_o} \cong -J\omega C \times \frac{Z_o}{2} \qquad (5)$$

Assuming the reflection ρ_1 is capacitive, the capacitance we want to measure is

$$C_1 \cong \frac{2|\rho_1|}{2\pi F_1 Z_o} \qquad (6)$$

The mechanical scaling we must use is the ratio of the capacitance we want to measure to the minimum we can detect. This is just the ratio of equations (4) and (6) giving

$$\text{SCALING FACTOR} = \frac{2\pi F_1 C_{MIN}}{|\rho_1|} \times \frac{Z_o}{2} \qquad (7)$$

Application to Directional Couplers

A problem in high performance directional couplers is to maintain the proper impedance in all regions of the coupler. The other problem here is one of being able to resolve the different regions of the coupler on TDR.

One requirement that was set on the measurement problem was that of being able to detect a reactive discontinuity giving a $\rho_1 = 0.005$ at 8 GHz.

Substituting these values into equation (7) gave a Scaling Factor of ten. Figure 2 is a picture of the scaled coupler. The total length (excluding the coaxial portion) is 22 inches or only 2.2 inches in the 1X model.
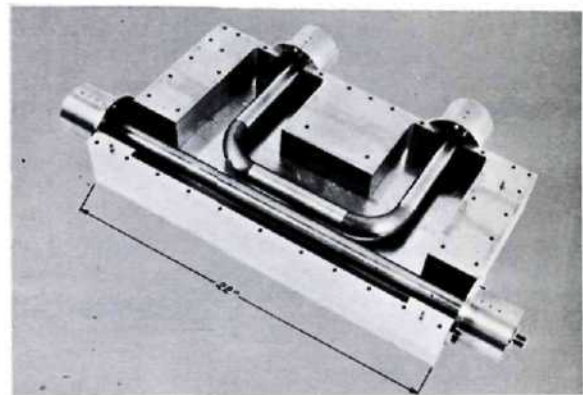

Figure 2.   10 Time Scale Coupler

Figure 3 is the TDR plot of half the coupler with the horizontal scale being 3 centimeters of coupler per centimeter of display. Complete resolution is possible for discontinuities 1-1/2 divisions apart on the scope face. This corresponds to 0.18 inches when scaled back to the original 1X model. Note that the total display of Figure 3 represents just over half the distance necessary for complete resolution of discontinuities in the 1X model. The 30 cm of display
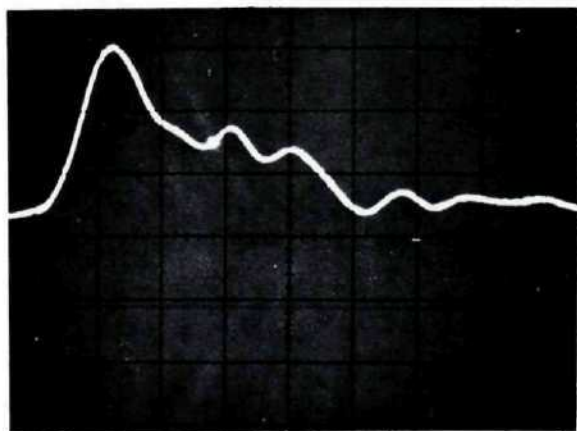
18

Figure 3. Coupler TDR Response
(3 cm/cm of Display, $P = .01$/cm)

Figure 4. Illustration of Moding Effects
(60 cm/cm of Display, $P = .01$/cm)

would become only 3 cm on the 1X model. Thus, the information in Figure 3 would be impossible to obtain from the 1X model.

MEASUREMENTS ON A MECHANICALLY SCALED MODEL

The following comments apply to all TDR measurements. With mechanical scaling these effects become even more important.

Basic Differences Between TDR and Single Frequency Measurements

In TDR measurements a step function serves as the signal source. The step function has a frequency spectrum which extends over a wide frequency range. The frequency spectrum of a zero rise time step decreases at 6 db per octave.[5] The frequency spectrum of a step function with an RC rise time of $1/\alpha$ is

$$F(P) = \frac{\alpha}{P(P + \alpha)} \qquad (8)$$

The frequency spectrum of (8) decreases at 6 db per octave to the point where $P = \alpha$ and decreases at 12 db per octave for $P > \alpha$. For the step generator in the 1415 (rise time = 50 picoseconds) the frequency spectrum begins to fall off at 12 db per octave starting at 20 GHz.

In the conventional system of swept or fixed frequency measurements the highest frequency of excitation is under the control of the operator. As is seen from equation (8) this is not true with TDR measurements.

Excitation of Resonant Modes with TDR

Since the driving function in TDR, the step function, has a wide frequency spectrum, resonant modes are excited. Because the sampling scope does not have a sharp cutoff in its frequency response it will respond to these resonances.

Figure 4 illustrates the appearance of this phenomena. The bottom trace illustrates a "normal" response. The 10X model is displayed from 0.8 to 2.4 divisions from the left of the scope face. When a perturbation is introduced into such a structure for matching purposes higher order modes may be excited. The effect is illustrated in the top trace. A load
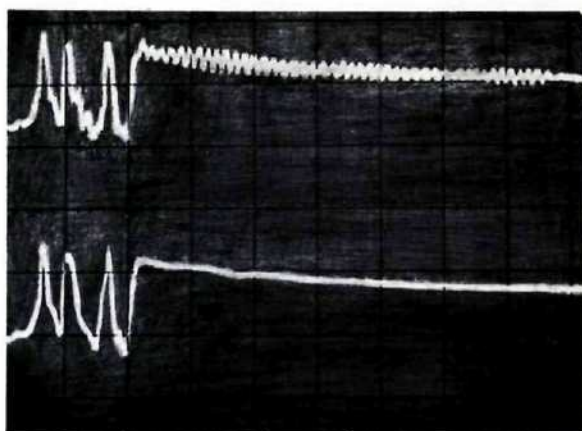
terminates the coupler and ideally there should be no further signal beyond the coupler as in the bottom trace.

The horizontal scale actually represents the time for the measurement step to pass the sampling point, be reflected from a discontinuity, and return to the sampling point. By counting the cycles per centimeter in the top trace one can determine the wavelength and frequency of the resonant mode.

$$\lambda_{RES} = \frac{2000 \text{ (cm of line/cm of display)}}{\text{No. of full cycles}}$$

$$F_{RES} = \frac{\text{Velocity in medium}}{\lambda_{RES}}$$

The bottom trace of Figure 5 is a portion of the coupler. In the top trace a tuning screw has been used to introduce a capacitive discontinuity into the coupler at the beginning of the trace. With no moding the remainder of the trace would be unaffected except for second order effects of multiple reflections.[1]

Figure 5. Moding Effects from Capacitive Tuning Screw (6 cm/cm of Display, $P = .01$/cm)

Correlation of Moding Effects with Swept Frequency Measurements

If moding is occurring within the coupler one should be able to detect it by measuring the coupler insertion loss. Figure 6 is a sweep frequency plot
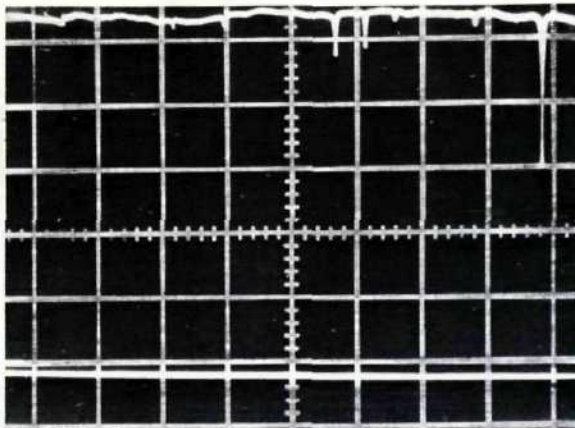
Figure 6. Swept Frequency Insertion Loss from 1 to 2 GHz

with the sweep going from 1 GHz to 2 GHz, left to right. A careful examination of this plot will show that there are ten distinct resonances.

Means of Eliminating Moding

There are three techniques for eliminating moding effects. These are: reducing the structure size so that moding cannot occur, introducing loss which couples selectively to the unwanted modes, and finally being careful not to excite the modes in the first place.

Reducing Structure Size. When one has already scaled up the size in order to make measurements this is not a practical solution here.

Introducing Selective Loss. Since the desired mode for TDR measurements is the TEM this is a good solution. Figure 7 is a repeat of Figure 4 with poly-iron lossy material in the region of the secondary arm. An examination of Figures 4 and 7 illustrates that the main line impedance was unaffected. This technique works by reducing the Q of the higher order modes.
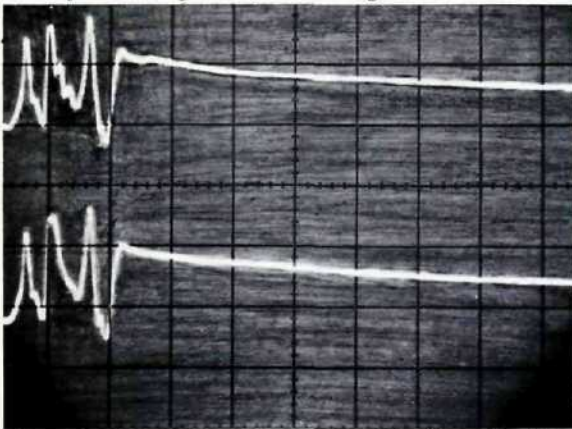

Figure 7. Mode Damping with Selective Loading

Figure 8 is a repeat of Figure 6 showing that on a swept frequency basis the modes have also been damped out.

For the TEM mode the current in the center conductor is axial. A possible means for selective mode loading would be to cut longitudinal slots and load them with polyiron. At this writing there has not been time to try this.
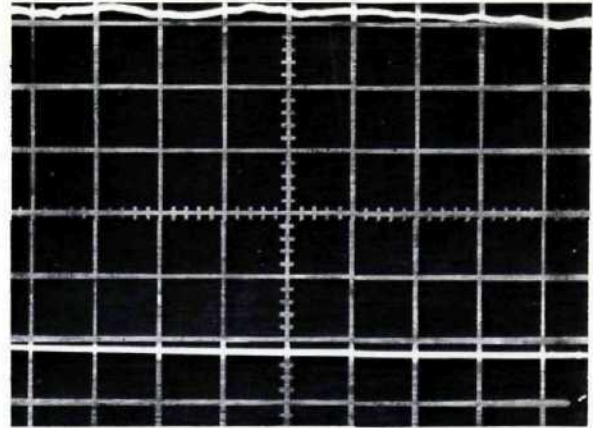

Figure 8. Swept Frequency Insertion Loss from 1 to 2 GHz with Selective Loading

Don't Excite the Modes. This is certainly the best solution. TDR offers an excellent tool for determining what type of compensation causes moding. However, in most practical design situations it is not possible to completely eliminate the excitation of other modes. A final solution should involve a combination of the last two methods.

CONCLUSIONS

As a result of working with this 10X coupler the author is convinced that where possible it is desirable not to scale by more than 5X. Others working in the microwave division concur in this. The problem is to keep the moding as high in frequency as possible.

Consider scaling a coax device normally built in 7 mm coax. The first mode occurs at approximately 18 GHz. 10X scaling brings this down to 1.8 GHz. A 5X scaling would raise this to 3.6 GHz. Thus 5X scaling reduces the energy in the step at the moding frequency (equation 8). In addition the measuring system frequency response is falling off.

Mechanical scaling combined with TDR offers many advantages to the designer. It allows accurate measurements of small reactive discontinuities at an equivalent frequency dependent only on the discontinuities which would otherwise be unresolvable. Finally, it has advantages comparable to swept frequency testing in indicating the presence of moding over very wide frequency ranges. A good design (independent of TDR) is one which does not excite higher other modes.

ACKNOWLEDGEMENTS

REFERENCES

1. B. M. Oliver, "Time Domain Reflectometry", Hewlett-Packard Journal, Vol 15, No. 6, February 1964.

2. "Time Domain Reflectometry", Application Note 62, Hewlett-Packard Company.

3. J. R. Whinnery and H. W. Jamieson, "Equivalent Circuits for Discontinuities in Transmission Lines", Proceedings of the IRE, February 1944.

4. J. R. Whinnery, H. W. Jamieson, and Theo Eloise Robbins, "Coaxial Line Discontinuities", Proceedings of the IRE, November 1944.

5. "Table of Important Transforms", Hewlett-Packard Journal, Vol 5, No. 3-4 1953. (Also reprinted in expanded form.)

SOME USES OF
TIME DOMAIN REFLECTOMETRY (TDR)
IN THE DESIGN OF
BROADBAND UHF COMPONENTS

by
Carl G. Sontheimer

Anzac Electronics, Inc.
Moody's Lane, Norwalk,Connecticut

With Permission of
Anzac Electronics, Inc.

SOME USES OF TIME DOMAIN REFLECTOMETRY (TDR) IN THE DESIGN OF BROADBAND UHF COMPONENTS

by

Carl G. Sontheimer

Anzac Electronics, Inc.
Moody's Lane, Norwalk, Connecticut   06851

SUMMARY

Time domain reflectometry (TDR) provides convenient and rapid guidance in the design of passive broadband UHF components. Typical instances include impedance transformers, balanced mixers, hybrid junctions, and the evaluation of ferrite toroids. The technique has also been of exceptional value in the testing and troubleshooting of subassemblies.

SCOPE

This paper presents some examples of the use of TDR as a qualitative guide for component design within a small commercial laboratory. The TDR system we use has a rise time of 130 picoseconds. Our organization is engaged in the development and manufacture of broadband passive devices. These span a frequency range from a few megacycles to S band. The building blocks used in this work are microstrip transmission lines, miniature coaxial cables, and ferrite toroids.
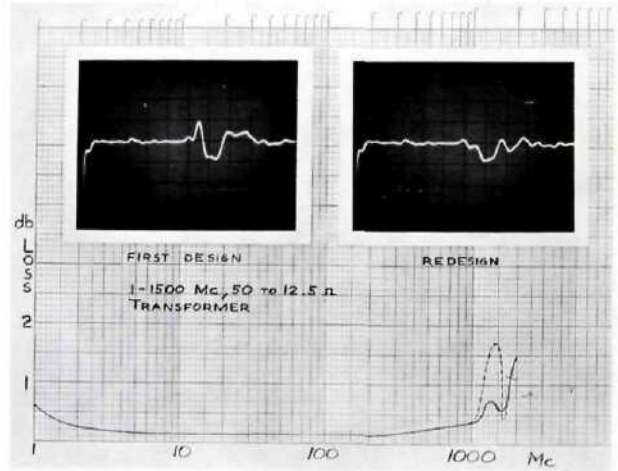

Figure 2. TDR Waveforms and Frequency Response of Broadband Transformer

USE OF TDR IN THE DESIGN OF A BROADBAND TRANSFORMER

The recent design of a 50 ohm-to-12.5 ohm transformer illustrates how TDR can expedite work on such components. The basic circuit, shown in Figure 1, is a transmission line transformer, consisting of two lines connected in series at input, and in parallel at the output. The impedance of these lines should be 25 ohms. The outer conductor of one line is above ground at the output. Ferrite toroids strung on this line provide the required common mode isolation. The coverage required of this transformer was 1 to 1,500 mc, with a loss not to exceed 1 db.

Figure 1 also shows in exploded view the printed circuit configuration and the transitions between stripline and coaxial line. In such layouts, the spacing between grounded and hot lands is critical.

The upper left-hand waveform in Figure 2 shows the reflection from the first breadboard model of this transformer. There is an inductive
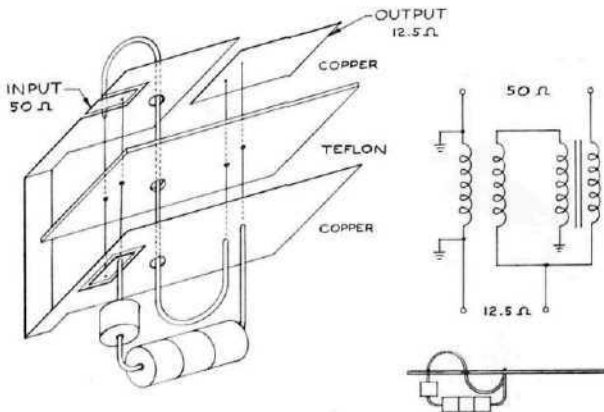

Figure 1. Schematic and Layout of 50 Ohm-to-12.5 Ohm Transformer
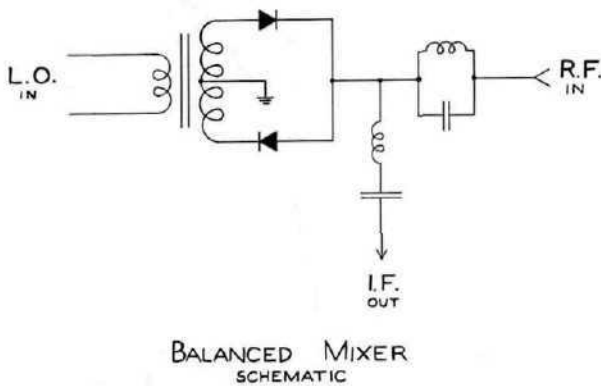
BALANCED MIXER
SCHEMATIC

Figure 3.

peak at the input, which indicates excessive spacing around the land forming the series connection between the two transmission lines. The dip following this inductance is attributable to the use of a transmission line with a characteristic impedance of 22 ohms instead of 25 ohms, which was not available. Finally, the rise in impedance at the output of the transformer indicates that the 12.5-ohm output stripline is too narrow.

The measured response of the transformer was satisfactory except for the 1.7-db peak of loss at 1,450 mc, shown in dotted lines on the graph.

A second breadboard was constructed, with narrower gaps around the series connection land at the input, and a broader output line. The response of this transformer is shown by the solid line on the graph. It meets the specification requirement. The response would no doubt extend higher in frequency if a 25-ohm transmission line were used.

In this case, the use of TDR probably reduced the total design time by at least two to one.

USE OF TDR IN BALANCED MIXER DESIGN

Figure 3 shows the basic schematic of one kind of balanced mixer. The diodes act as a switch, ideally open-circuited when the diodes are back-biased, and ideally providing a short to ground when the diodes are conducting. Both tuned circuits are resonant at the intermediate frequency. The series circuit prevents signal power from being dissipated in the I.F. load.

The parallel circuit blocks transmission of I.F. energy to the signal source impedance. Except for diode resistance and capacity, the principal factors limiting the performance of a practical broadband mixer are leakage inductance in the transformer secondary, which adds to the resistances of the diodes in the conducting state, and reflections generated in the signal input path by the two tuned circuits.

Figure 4 illustrates a use of TDR in the evaluation of balanced mixer designs. Each waveform shows the reflections from the signal port of a mixer with the diodes alternately back- and forward-biased. The two upper waveforms were taken with a commercial mixer covering the range of 10 mc to 1 gc. In one case, 1N831 diodes were used and, in another, hot carrier diodes. The greater on-off impedance variation obtained in this case with hot carrier diodes is evident.

The waveform also shows an inductive reflection immediately preceding the diodes. This observation caused design effort to be concentrated on the signal input circuits, with the result shown in the lower waveform. In this mixer, the inductive discontinuity has been greatly reduced, and low conversion loss is obtained over the range from a few megacycles to 2.4 gc.

The TDR equipment has also proved useful in guiding efforts to improve L.O.-to-signal isolation. This is necessary for local oscillator noise reduction and low noise figure. In this case, transmission rather than reflection is used, as shown in Figure 5. The purpose of the attenuator is to reduce the diode current caused by the inci-
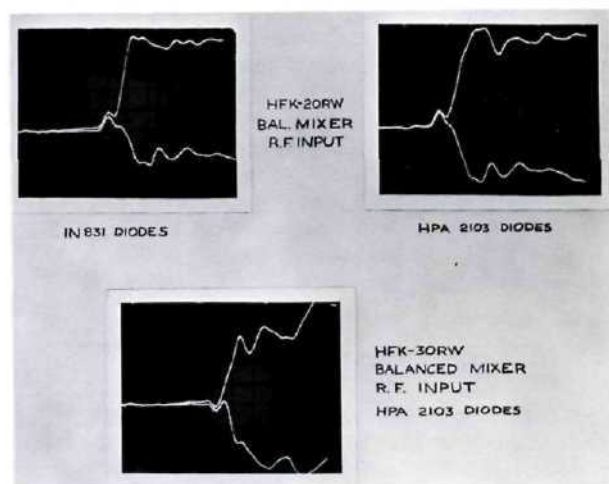

Figure 4.   Reflections from Signal of
Balanced Mixer

dent pulse to an order of magnitude below the diode biasing current.

Typical waveforms are shown in Figure 6. The upper trace was made with the diodes back-biased, and the lower trace with the diodes conducting. Very nearly identical traces were obtained with different sets of diodes, indicating that the feed through is due to capacitive and inductive unbalance in the transformer driving the diodes. The left-hand picture was obtained with the 10-to-1,000 mc mixer referred to earlier. Using such pictures as a guide, work was concentrated on the transformer. The right-hand picture in Figure 6 shows the results achieved in a new mixer, with an upper frequency limit of 2,400 mc. Conventional measurements show isolation improved by 10 to 15 db.

USE OF TDR IN HYBRID JUNCTION DESIGN

These junctions have 0-degree or 180-degree phase shift between outputs, and are related to magic tees rather than to quarter-wave hybrids.

In a practical device, the proper characteristic impedances must be preserved everywhere, from the connector to the stripline and through the transitions from stripline to coaxial line. Size must be minimized by keeping all stripline paths as short as possible. The separation between nodes is then beyond the resolution of the TDR system.

In such cases, useful information can be obtained from an expanded unit, in which all nodes and transitions are separated by at least 2 inches. Figure 7 shows a commercial hybrid junction with a range of 2 to 2,000 mc, and an expanded breadboard version of the same device. Figure 8 shows the reflection from the sum ports of both units. The input and output connectors of both models have been deliberately mismatched to indicate their locations.

The upper trace corresponds to the standard device, and the lower trace to the expanded one. Appreciable mismatches are immediately apparent in the lower trace, which reveals both their location and their magnitude, thus indicating what must be done to correct them. In this case, touching the unit showed that the coaxial impedances were correct, but the stripline interconnections had to be widened. None of this information is available from the reflection of the standard unit, which is actually misleading in its relative smoothness.

When the nature of the device does not permit making an expanded model, or when the frequency
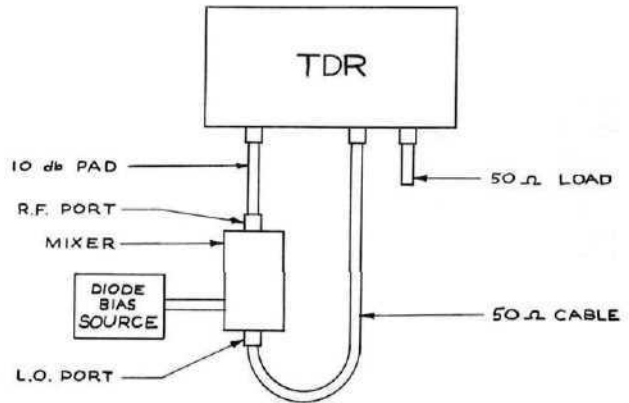

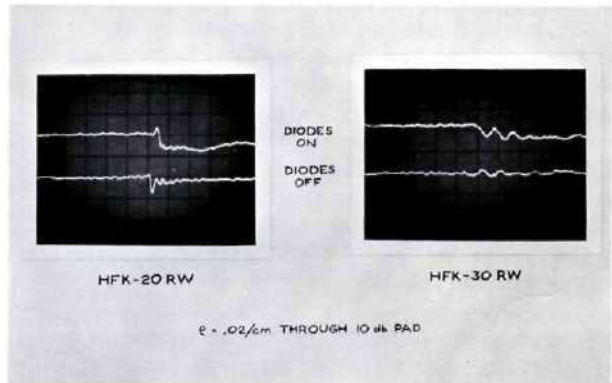Figure 5. Block Diagram of Isolation Test Setup

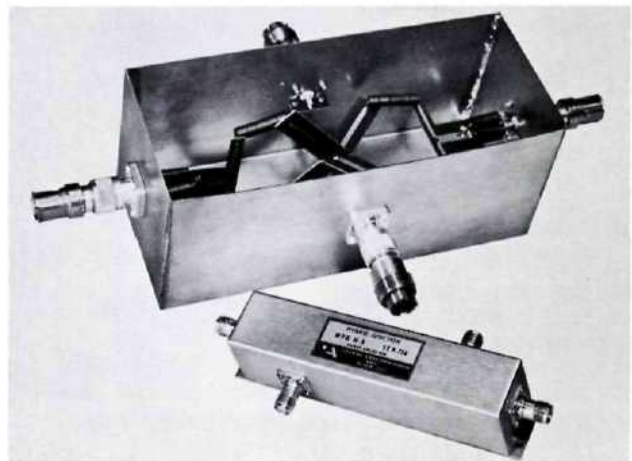Figure 6. Local Oscillator-to-Signal Port Transmission in Balanced Mixer

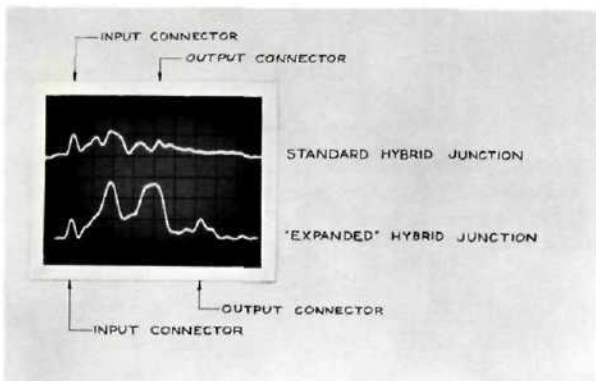Figure 7. Commercial Hybrid Junction and Expanded Model for TDR Studies

Figure 8. Reflections from Standard and Expanded Hybrid Junctions

range of interest too high for the present TDR state of the art, one can resort to models scaled down in frequency. The knowledge thus gained can then be applied to the actual device.

TDR in the transmission mode is a useful tool for study and analysis of the isolation of hybrid junctions. The circuit arrangement is the same as that shown earlier for the balanced mixer, except that no pad is needed.

The upper trace of Figure 9 shows signal transmission through two isolated ports of a 2-to-1,000 mc hybrid. An internal adjustment has been set to yield a waveform consisting of three peaks of equal amplitude, with the center peak reversed in phase. This provides good isolation at lower frequencies. This is shown in the lower trace in Figure 9. Here a 1-gc low pass filter has been inserted ahead of the hybrid junction. No evidence of feed through is apparent in the display, even at maximum gain. The measured isolation is in excess of 40 db at 1 gc, and increases with decreasing frequency.

Use of TDR equipment in the transmission mode also enables immediate identification of the phase reversing paths between ports of hybrid junctions and related networks.

USE OF TDR IN MATERIAL EVALUATION

TDR has provided an accurate and rapid method of testing ferrite toroids for two important parameters: shunt resistance and shunt inductance.

Figure 10 shows a toroid test jig consisting of a modified TNC connector. The rear cap is re-

moved, the toroid under test is inserted and the cap replaced. The test jig is then attached to the output of the TDR unit.

Figure 11 shows typical displays. Using a fast sweep -- usually 0.2 nc/cm, the reflection coefficient of the toroid is obtained, and its shunt resistance is calculated as shown in the figure. The vertical gain is then adjusted to place the beginning of the bead reflection to 10 cm above the base line. Sweep speed is reduced so that most of the *exponential decay can be seen.* The time required for the exponential to decay to 37 percent of its initial height, multiplied by the parallel resistance of the 50-ohm line and the ferrite shunt resistance, is the shunt inductance of the bead. The computation is shown in Figure 11 for a commercially available filtering bead.
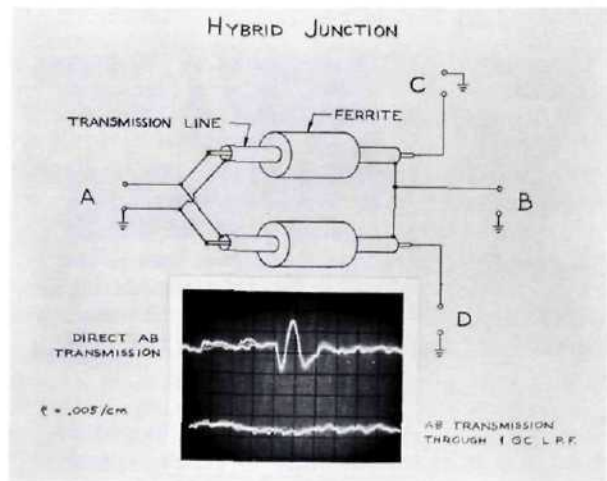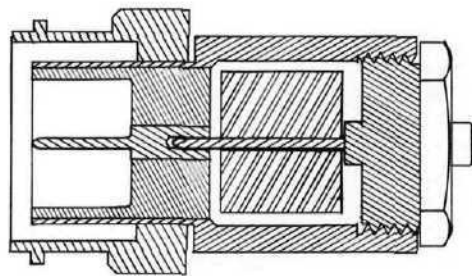

Figure 9. Signal Leakage between Isolated Ports of a Hybrid Junction

FERRITE BEAD TEST JIG

Figure 10. Ferrite Toroid Test Jig

The results computed from these rapid TDR measurements check within 5 percent with those obtained from more laborious procedures.

SOME USES OF TDR IN SUBASSEMBLY TESTING

One pair of ports in all 180-degree hybrid junctions has twice the impedance of the other pair. Two-to-one impedance transformers must be used to correct for this. The transformer we have developed for this purpose -- which has a bandwidth of 2 mc to 2 gc -- has ten transitions between the printed circuit board and the coaxial lines. It is important to verify correct operation of the transformer subassemblies before wiring them into the completed hybrid junction. TDR has enabled us to verify correct operation in a few seconds, and also to locate the fault in a defective transformer much more quickly than by any other means.

Figure 12 shows the very simple jig used for this purpose. Figure 13 shows a transformer subassembly inserted in the jig. The waveform is inspected first with the transformer output open, and then with the output shorted. If the trace deviates from the norm in either test, the waveform is compared against a chart like the one shown in Figure 14.

This chart was prepared by deliberately introducing, one after the other, every short possible in one section of the transformer. The tester compares the waveform on the 'scope with those on the chart, identifies the corresponding picture, and tags the transformer with the appropriate notation.

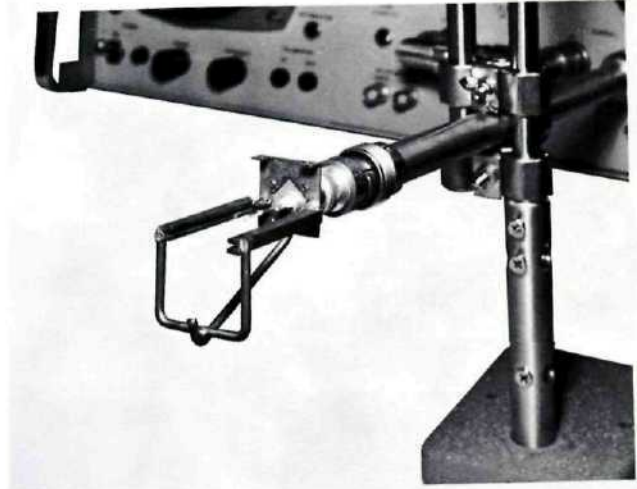Before this test was available, defective

Figure 12. Test Jig for Transformer Subassembly

Figure 13. TDR Test of Transformer Subassembly

transformers were discarded, because it cost more to troubleshoot and repair them than to build new units.

REACTION OF NON-PROFESSIONAL EMPLOYEES TO TDR

An unexpected dividend is the increased interest and output which TDR has brought about in our technicians. It gives them a physical picture which they rapidly learn to interpret, and has stimulated a number of excellent suggestions and inventive ideas. Some of our production girls have also learned to use the equipment for go-no go tests.

$$10 \text{ cm STEP} \qquad 2 \text{ ns/cm}$$

$$R = Z_o \frac{1+\rho}{1-\rho} \qquad L = \frac{RZ_o}{R+Z_o} \tau = \frac{89 \times 50}{139} \times 50$$

$$= 50 \left(\frac{1.28}{.72} \right) = 89 \, \Omega \qquad = 115 \times 10^{-9} = .115 \, \mu h$$
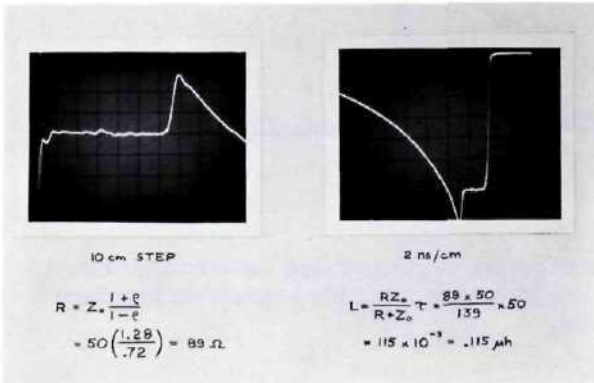
Figure 11. Ferrite Test Waveforms and Computations

H-8/H-9 TRANSFORMER CARD

ALL PICTURES 4 cm. STEP
1 ns/cm

SECOND PEAK 1.5 DIVISIONS HIGH. SMALL NEGATIVE BUMP BETWEEN THE TWO PEAKS

"A" LINE SHORTED AT OUTPUT

SECOND PEAK IS ROUND AND 0.8 DIVISIONS HIGH

SHORT AT INPUT TO "A" LINE

ALL O.K.

SECOND PEAK 1.7 DIVISIONS HIGH. NO NEGATIVE BUMP

2 OUTPUT LANDS SHORTED ON BOTTOM OF BOARD

SECOND PEAK IS POINTED AND 0.8 DIVISIONS HIGH

SHORT AT INPUT TO "B" LINE

NEGATIVE PEAK 1.2 DIVISIONS BELOW STARTING LINE

"C" LINE SHORTED AT CONNECTION END

SECOND PEAK 2.0 DIVISIONS HIGH AND POINTED, WIGGLE BETWEEN THE TWO PEAKS

"B" LINE SHORTED AT OUTPUT

SECOND PEAK IS VERY POINTED AND 1.2 DIVISIONS HIGH

SHORT TO GROUND AT INPUT TO "C" LINE

NO NEGATIVE PEAK

"C" LINE SHORTED AT OUTPUT END

SECOND PEAK 2.0 DIVISIONS HIGH. NO WIGGLE BETWEEN PEAKS

2 OUTPUT LANDS SHORTED ON TOP OF BOARD
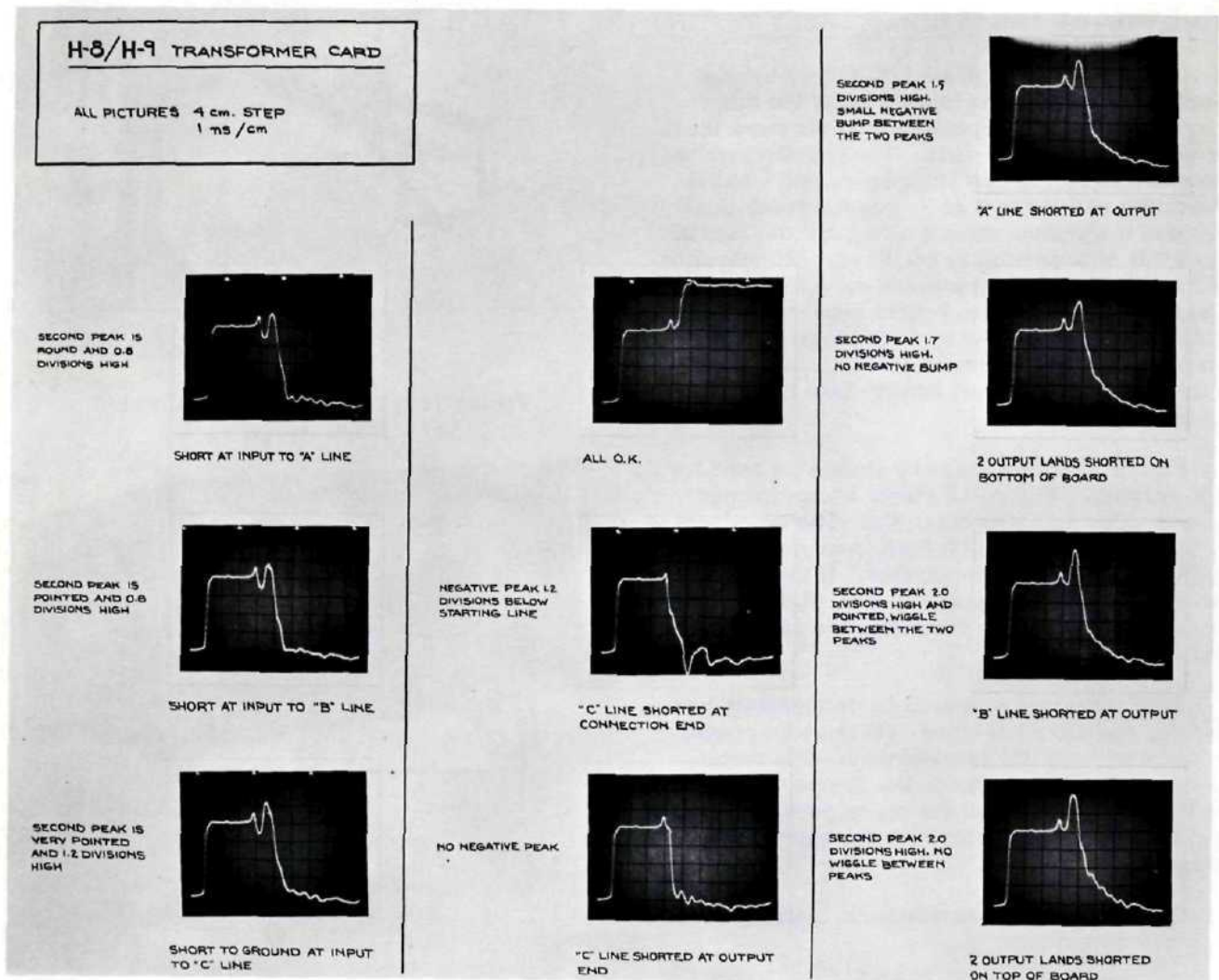
Figure 14. Troubleshooting Chart for Transformer Subassembly

CONCLUSIONS

TDR has greatly accelerated our development, design, and production test work, with a corresponding decrease in costs. It is a powerful tool for qualitative analysis, and an excellent indica-tor of where to concentrate development effort. It is also a very valuable production test instrument.

THERMOCOUPLE FAULT LOCATION BY TIME DOMAIN REFLECTOMETRY

by
D. B. Martin and A. J. Otter

Atomic Energy of Canada Limited
Chalk River, Ontario

With Permission of
Atomic Energy of Canada Limited

THERMOCOUPLE FAULT LOCATION BY TIME DOMAIN REFLECTOMETRY

by

D. B. Martin and A. J. Otter

SYNOPSIS

The application of Time Domain Reflectometry for fault finding in thermocouple circuitry has been investigated. This technique consists of applying a fast rise pulse to the thermocouple and observing the reflections with a sampling oscilloscope. The pattern and position of the reflected pulse depend upon the fault.

A metal sheathed thermocouple acts as a lossy transmission line; consequently, the reflected wave is nearly exponential. Extension wire is also lossy and, if unshielded, its stray capacitance and inductance affect the pulse propagation velocity. The velocity must therefore be determined for each installation.

The method is suitable for identifying faults. For accurate location, it is necessary to compare the fault reflection with a reference obtained from an identical sound thermocouple or from the same thermocouple at installation. If such a comparison is possible, we estimate that fault location is typically accurate to within $\pm 10\%$ for circuits with up to 75 ft of unshielded extension wire and 25 ft of sheathed thermocouple 1/16 in O. D.

TABLE OF CONTENTS

Page

1. INTRODUCTION

Metal sheathed thermocouples are extensively used in reactors for temperature measurements. When faults such as open or short circuits or breakdown of insulation between the sheath and the inner conductors develop, conventional methods of fault detection (i.e., measurements of loop and insulation resistance) do not always define the fault. For example, an open circuit in an extension wire, which could be replaced, is indistinguishable from an open circuit in the thermocouple, which may be impossible to replace.

The Hewlett-Packard Co. has developed equipment for an advanced technique of transmission line testing which they have termed Time Domain Reflectometry or TDR. In a reflection system analogous to radar, a fast-rise pulse (less than one nanosecond) is applied to the transmission line. This wave front propagates along the line at a velocity fixed by the line characteristics. Any impedance discontinuity on the line causes a reflected wave to travel back towards the generator; this reflection indicates the type of discontinuity and its location. In coaxial cable, short circuits, open circuits and other discontinuities can be located within 0.5 in.

We have investigated this technique for locating faults in metal sheathed thermocouples using the equipment and methods developed by Hewlett-Packard [1]. For completeness, these methods are described with additional procedures which we found useful.

2. EQUIPMENT

The equipment necessary for TDR is described in Hewlett-Packard publications [2]. We used a model 185 Hewlett-Packard sampling oscilloscope with a type 187B plug-in amplifier and 213B pulse generator.

The system rise-time observed with the sampling oscilloscope was about 350 ps and its magnitude 350 mV. Initially, a model 213A pulse generator having a source impedance of three ohms was used, but multiple reflections due to severe impedance mismatch caused difficulty in interpreting the reflection. This difficulty was solved by using a type 213B generator with an internal impedance of 50 ohms.

Permanent records of the reflection patterns were obtained from the oscilloscope with a Moseley X-Y recorder.

3. THEORY

The following theory for low-loss transmission lines may be supplemented from standard transmission texts such as reference 3.

Figure 1 is the classical model of a transmission line considered as a distributed filter with constant parameters.

By solving the nodal differential equations [3], one obtains for an infinite line:

$$Z_0(s) = \frac{e_i}{i_i} = \left[\frac{R+sL}{G+sC}\right]^{1/2} \quad (1)$$

where $Z_0(s)$ is defined as the characteristic impedance

and s is the Laplace derivative operator (sometimes written as p).

Use of the Laplace operator rather than the familiar $j\omega$ operator for steady state sinusoids permits transformations from the frequency domain to the more useful time domain.

For low-loss lines where R and G are small, Equation 1 may be simplified for high frequencies to:

$$Z_0 = \left[\frac{R+sL}{G+sC}\right]^{1/2} = \left[\frac{L}{C}\frac{1+\frac{R}{sL}}{1+\frac{G}{sC}}\right]^{1/2} = \left[\frac{L}{C}\right]^{1/2} \quad (1a)$$

since $R \lesssim sL$ and $G \lesssim sC$.

At any point where the line impedance has changed to $Z_r (\neq Z_0)$, a portion of the incident pulse energy returns towards the source as a reflected wave. Its magnitude relative to the incident wave is defined by a reflection coefficient:

$$k_r = \frac{e^-}{e^+} = \frac{Z_r - Z_0}{Z_r + Z_0} \quad (2)$$

where e^+ is the incident voltage wave,

and e^- is the reflected voltage wave.

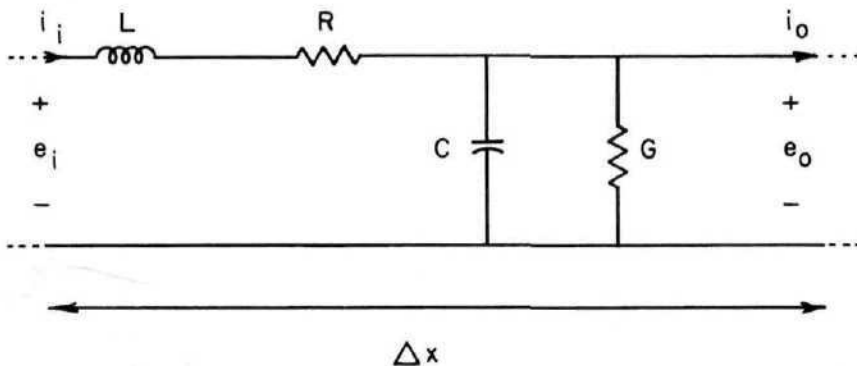The sign of k_r depends upon the value of Z_r relative to Z_0.

Figure 1. Transmission Line Model

The oscilloscope at the input displays the incident wave step. After a time delay T, the reflected wave of height e^- is superimposed upon the generator voltage, and the observed wave is the sum of the incident and reflected waves. Since the incident wave must travel to the discontinuity and the reflected wave must travel back before detection, the time delay between the incident pulse from the generator and the reflection is:

$$T = \frac{\text{total distance travelled}}{\text{pulse velocity}} = \frac{2\,l}{v}$$

where l is the length of the line,
and v is the wave velocity.

If the wave velocity is known from calculations or previous measurements, the distance to the impedance discontinuity can be determined from the measured time delay. If the incident wave voltage has unit amplitude, and the reflected wave has height k_r, total height after time T is;

$$h = e^+ + e^- - 1 + k_r \qquad (3)$$

Hence (2) may be rewritten to give,

$$Z_r = \frac{h}{2-h} Z_o \qquad (4)$$

Typical waveforms for a lossless transmission line terminated by resistive Z_r are shown in Figure 2.

If several impedance discontinuities are present, multiple reflections similar to those in Figure 3 may result.

The first reflection k_1 correctly defines the first discontinuity, but the next step, which is theoretically of height $k_2 (1 - k_1^2)$, may normally be considered as k_2; this is a close approximation if k_1 is small, i.e., the preceding mismatch is not too great. Multiple reflections are normally negligible, but their presence must always be considered.

If Z_r is complex, the reflections are exponential. Consider a case where Z_r is a resistor in series with a capacitor (Figure 4).

$$Z_r = R + \frac{1}{Cs} - Z_o$$

$$\text{and } k_r = \frac{e^-}{e^+} = \frac{R + \frac{1}{Cs} - Z_o}{R + \frac{1}{Cs} + Z_o} \qquad (5)$$

$$\text{where } Z_o = \left[\frac{L}{C}\right]^{1/2}$$

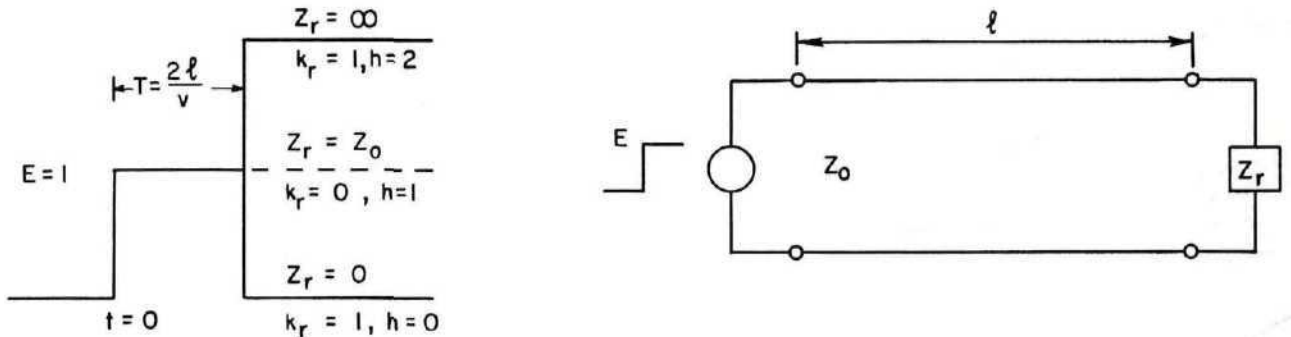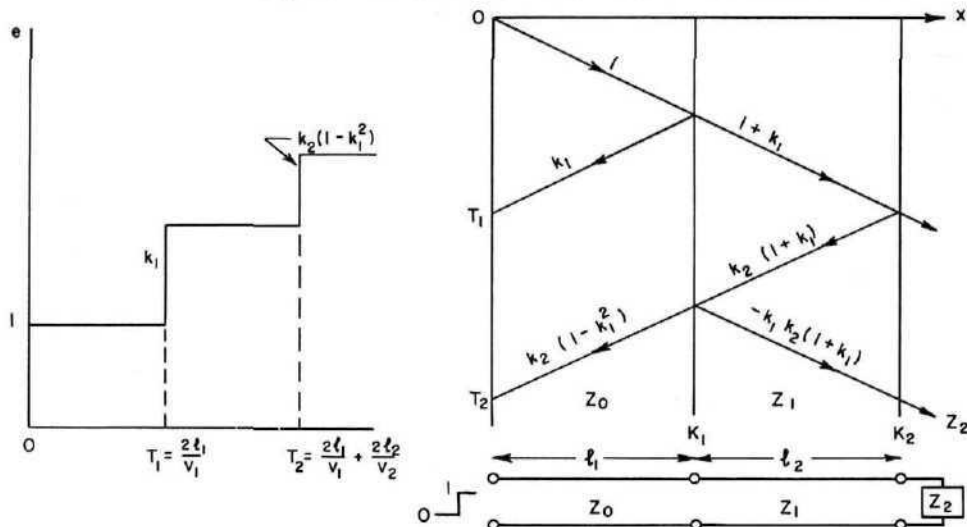

Figure 2. Reflection from lossless terminated line

Figure 3. Multiple reflections from lossless line

Let a voltage step E be applied, i.e.,

$$e^+(t) \approx E \text{ for } t \geq o, \text{ then } e^+(s) = \frac{E}{s}$$

$$\text{and } e^-(s) = \frac{E}{s} \cdot \frac{1 + C(R - Z_O)s}{1 + C(R + Z_O)s} \quad (6)$$

By Laplace transformation (3)

For $t \geq o$

$$e^-(t) = E\left[1 - \frac{2Z_O}{R + Z_O} \exp\frac{-t}{(R + Z_O)C}\right] \quad (7)$$

In this expression, the instant the pulse step reaches the lumped impedance Z_r is taken as $t = 0$

This case is important, for a thermocouple which is a lossy line can be considered as a series resistance and capacitor when t is small. The effective series resistance can be determined from the initial slope (Appendix A).

Thermocouples must be considered as lossy lines since their series resistance (especially for small sizes) is appreciable. For such lines the characteristic impedance is frequency dependent, the approximation $R \leq sL$ used in Equation (1a) is no longer valid, and mathematical solutions of the reflections are normally extremely difficult. However, the reflection from an infinite lossy line can be derived (2) as in Appendix B.

The reflection is given by:

$$f(t) = 1 - \left\{I_o\left[\frac{Rt}{2L}\right] + I_1\left[\frac{Rt}{2L}\right]\right\}\exp\left[\frac{-Rt}{2L}\right] \quad (8)$$

where $I_o\left[\dfrac{Rt}{2L}\right]$ and $I_1\left[\dfrac{Rt}{2L}\right]$

are modified Bessel functions of the first and second type respectively. The reflection voltage $f(t)$ gradually approaches unity, the reflection voltage for an open circuit. This expression is typical of the mathematics required even for simple lossy lines.
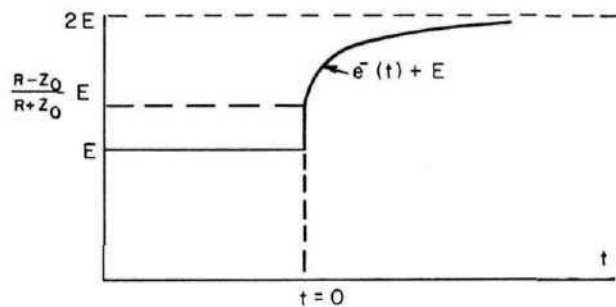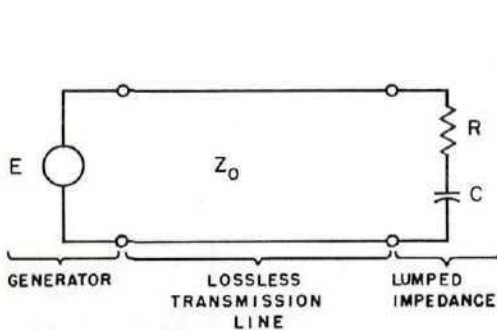
4. PROCEDURE

The thermocouple and test circuit considered in this investigation are shown in Figure 5.

This circuit can be considered as two lossy transmission lines connected in series and terminated in a short circuit at the junction which may or may not be joined to the sheath. In most thermocouple installations, the pulse was applied to one terminal of the extension wire with a short clip lead. The ground terminal of the generator was similarly connected to the other extension wire. The initial spike reflections due to the stray capacitances of these clip leads did not affect the reflections from the thermocouple.

The experimental procedure was divided into three phases:

(1) Tests with twin-conductor low-loss shielded cable to develop a familiarity with the equipment and techniques and to obtain ideal characteristics.

(2) Tests on thermocouples under laboratory conditions.

(3) Tests on thermocouples installed in NRU reactor.

5. RESULTS

5.1 Twin Conductor Low-Loss Cable

Various thermocouple configurations were simulated with twin conductor sheathed cable (type RG108A/U).

The reflection in Figure 6 is from such a cable with the sheath floating (i.e., no ground loop connection to generator). The reflection is the same whether the junction is grounded to the sheath or not. In thermocouple installations, the sheath is often grounded and will thus be connected in parallel with the thermocouple wire grounded at the generator. Figure 7 simulates this case for an ungrounded junction, and Figure 8 simulates the case with a grounded junction.

Because of the different line parameters, the characteristic impedance has decreased from 68 ohms

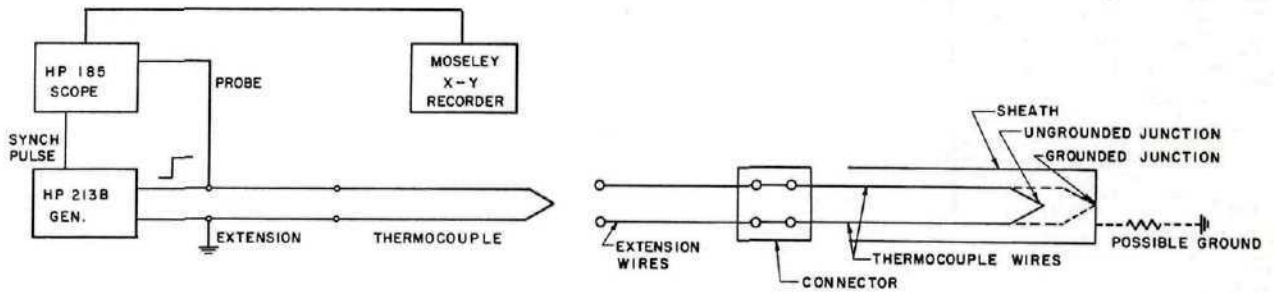Figure 4. Reflection from Line Terminated by Complex Impedance

Figure 5. Typical Thermocouple Circuit

(Figure 6) to 37 ohms (Figure 7). Also, the two conductors of the ungrounded cable (Figure 7) are effectively in series. Hence the step travels along both conductors in turn until reflected from the short circuit to the sheath at the generator ground. The spike at time T marks the local mismatch conditions due to stray capacitance and inductance at the junction of the two conductors.

The major difference between Figures 6 and 8

is a similar decrease in impedance again due to the differences in distributed L and C.

In practice, the grounded sheath situation of Figures 7 and 8 would only be approached if the ground loop acted as a short transmission line between the generator ground and the sheath. Thus, for the lossless cable used here, the impedance may vary from 37 to 68 ohms depending upon the nature of this ground loop.
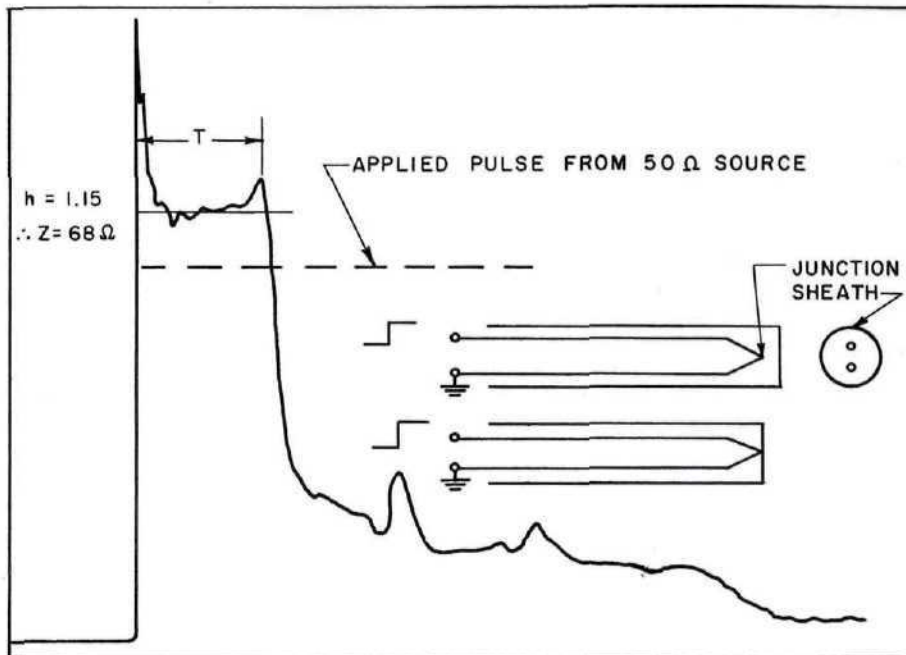

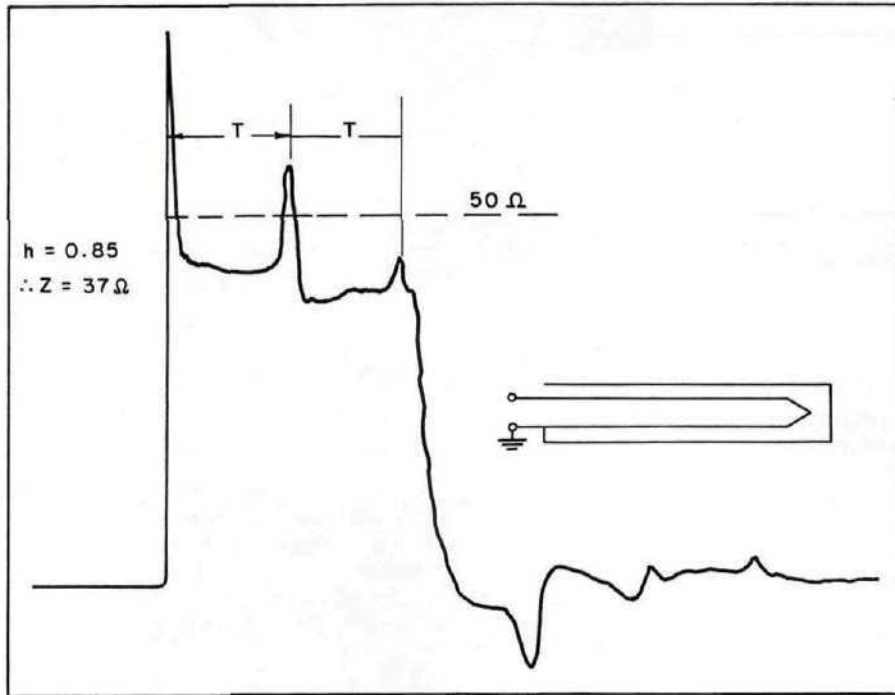Figure 6. Lossless Line with Floating Sheath

Figure   7.   Lossless Line with Grounded Sheath and Ungrounded Junction
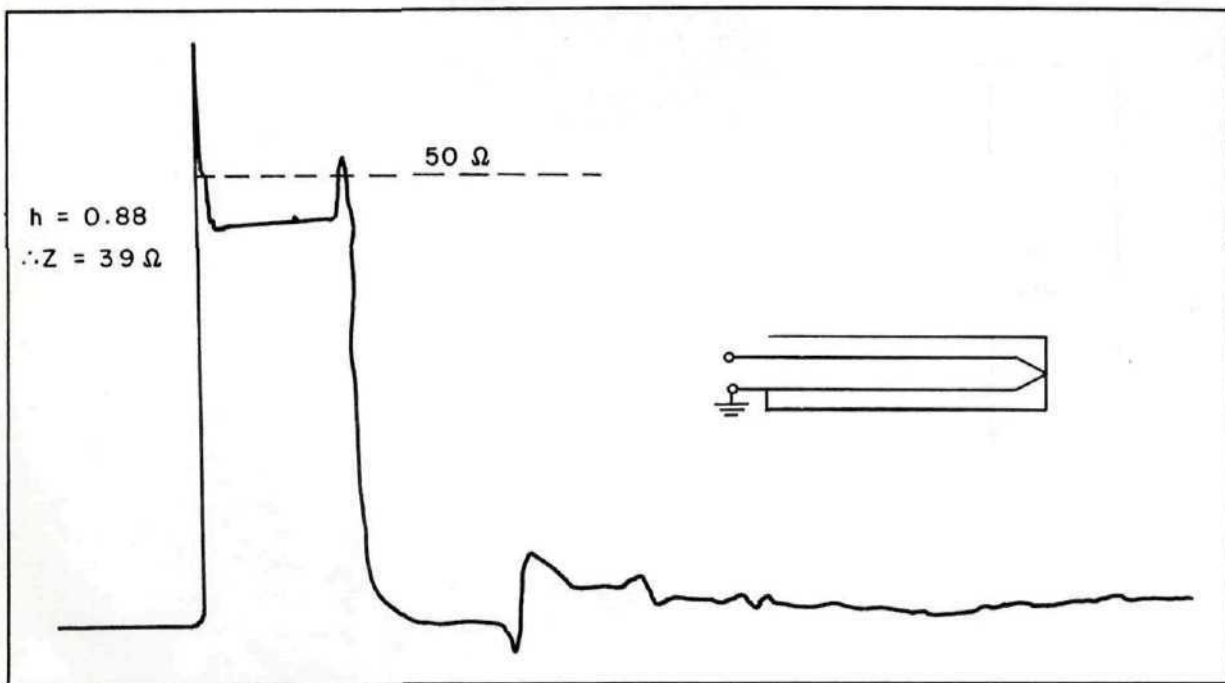

Figure   8.   Lossless Line with Grounded Sheath and Junction

5.2 Tests on Laboratory Thermocouples

The location of faults by TDR hinges on two factors:

(1) The attenuation due to lossiness of the thermocouple, which limits the length that can be usefully tested.

(2) The constancy of the wave propagation velocity which determines the accuracy with which faults can be located.

The distributed parameters of a sample 0.062 in O.D., sheathed, type K thermocouple were obtained by bridge measurements and from theoretical graphs[5].

TABLE 1

Parameters for 0.062 in. Thermocouple

	BRIDGE	WHEELER (REF. 5)
R	6.2Ω/ft	-
L	0.164μH/ft	0.204μH/ft
C	47.0 pF/ft	40.6 pF/ft
G	$\leq$ 7 x 10^{-12}mho/ft	-
Z_o	$=\left[\dfrac{L}{C}\right]^{1/2}$ 59Ω	70Ω

5.2.1 Effect of Series Resistance

This measured value of G, the shunt conductance, justifies the approximation that G= 0 and that the transmission losses are due to R, the series resistance. Using the relation developed in Appendix A and these measured values of L and C, the calculated series resistance is 9.1 ohms/ft. The apparent increase in R compared to Table 1 is probably due to the skin effect, which is difficult to evaluate for a step function which contains a wide band of frequency components.

In Figure 9, the reflection functions defined in the Appendices are plotted using the measured parameters and compared with an actual reflection produced by a 0.062 in. O. D. thermocouple. The theory gives a reasonable agreement but expressions for more complicated finite lossy lines have not been obtained. We have found the theory useful for qualitative understanding of the basic principles involved.

The effect of series resistance is shown in Figure 10 where the attenuation increases as the thermocouple size decreases.

Figure 11 shows reflections from ungrounded thermocouples with the sheath grounded or floating. The degeneration of the reflections compared to lossless line (Figures 6 and 7) is evident. Reflection B does exhibit a secondary reflection at time 2 T (not fully shown in Figure 11) but it is distorted by attenuation. The effective series resistance has been decreased as the grounded sheath acts as part of the transmission line. Only the upper part of the reflection is shown in this figure as the oscilloscope sensitivity has been increased.

The reflections shown in Figure 12 are for a typical thermocouple open circuited or shorted at the junction. These reflections therefore represent either a faulted or a normal thermocouple.

5.2.2 Effect of Extension Wire

Extension wire also attenuates the pulse, but its series resistance is usually less than that of the thermocouple, so the attenuation is less severe. Figure 13 is a reflection from a typical thermocouple with extension wire. The dashed reflection (A) is from the open circuited extension wire. Due to attenuation, the rise-time and amplitude of the wave reflected from the open circuit of the extension wire
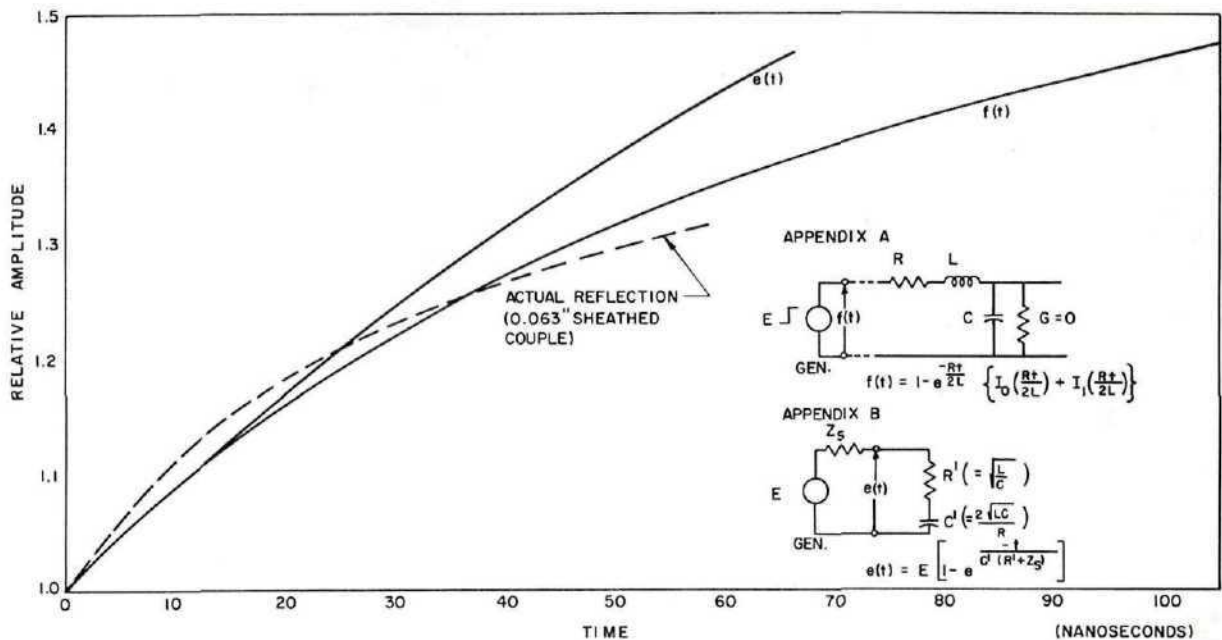

Figure 9. Theoretical and Experimental Reflections
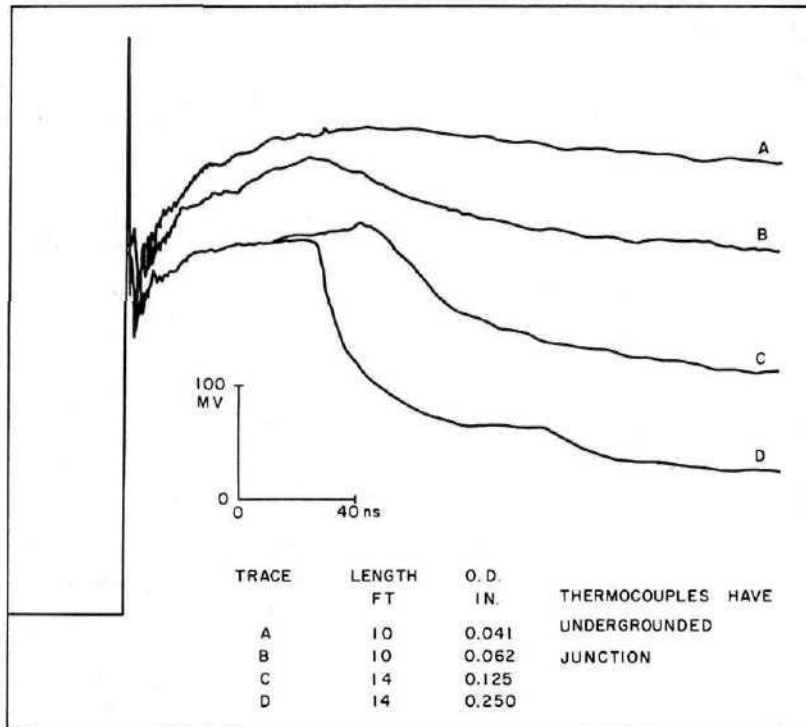Compared for a Lossy Thermocouple

Figure 10. Reflections from Thermocouples of Various Sizes
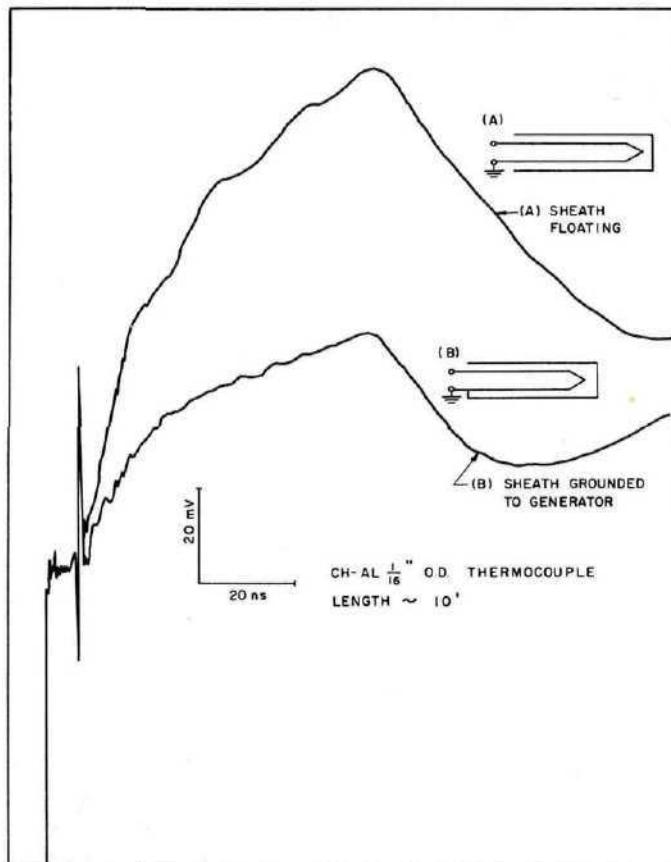

Figure -11. Two Types of Reflections from a Typical Thermocouple
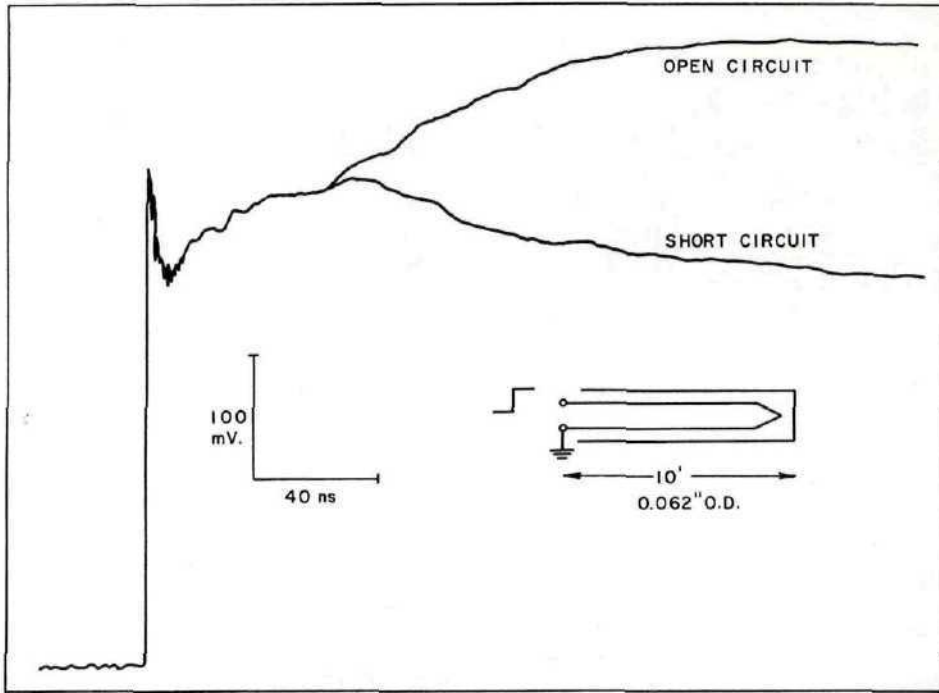
Figure   12.   Reflection from Typical Sheathed Thermocouple
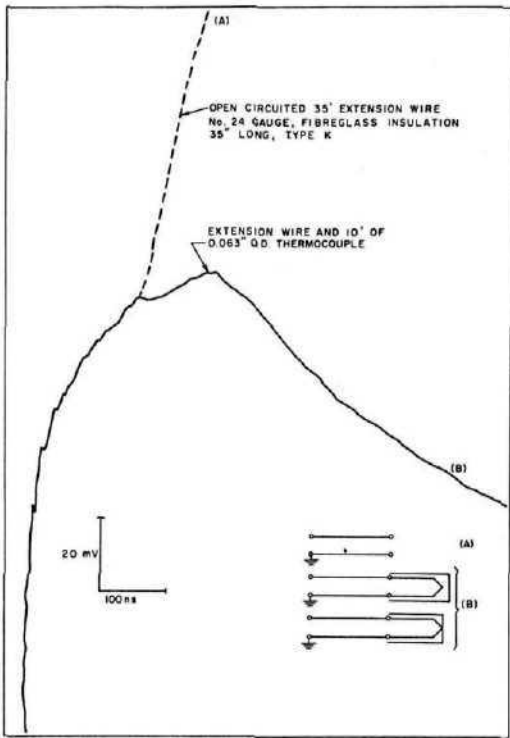

Figure   13.   Reflection from Thermocouple
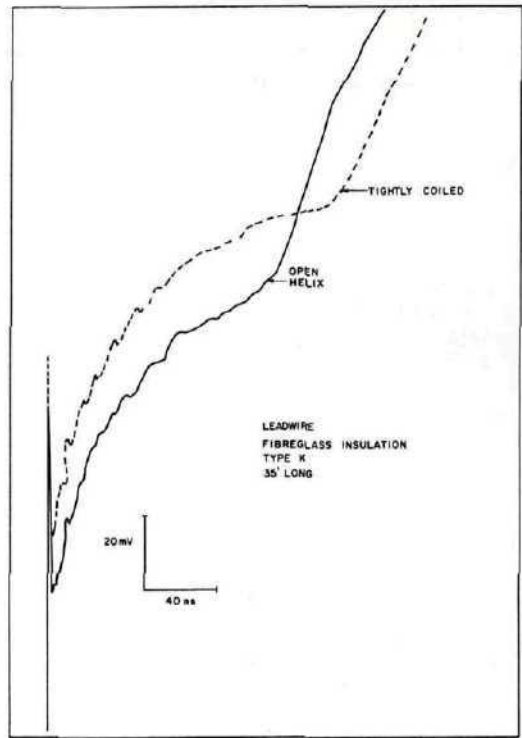Extension Wire

Figure   14.   Propagation Velocity
of Unshielded Lead Wire

are less than for the applied step. With the sheathed thermocouple connected to the extension wire, the incident step continues until reflected from the junction short circuit as shown by reflection (B). The additional attenuation by the lossy thermocouple causes this further degradation of the reflection.

The different characteristic impedance of the extension wire and the thermocouple cause the slight discontinuity in the waveform marking the end of the extension wire. Lossless reflections would be similar to Figure 3. The connectors (male-female plugs, terminal boards are spot-welded and potted in epoxy) between the extension wire and the thermocouple are too short to cause a detectable reflection from the attenuated incident wave.

The reflections do not change with grounded or ungrounded construction if the sheath is not connected to the generator ground. This agrees with the results from Figure 6.

5.2.3 Velocity of Propagation

The propagation velocity along a sheathed thermocouple is independent of the surrounding materials because of the shielding effect of the sheath. With unshielded extension wires, this lack of shielding causes considerable variation in the velocity due to variable stray effects. In Figure 14, for example, the velocity is 25% less for a tightly coiled extension wire than for an open helix. Thus the velocity for an installed lead wire connot be predicted, but is constant for a fixed installation. However, shielded extension wire exhibits a constant velocity regardless of installation.

The wire material also determines the pulse velocity, possibly due to variations in L from frequency effects. The velocity is about 20% less if the pulse is applied to the iron wire than if applied to the constantan wire of a type J thermocouple. It is therefore important to note the conductor polarity. For chromel and alumel, the velocities are nearly the same.

SUMMARY

(1)   Reflections from open circuits and short circuits can be clearly identified in normal thermocouple assemblies.

(2)   The velocity along unshielded extension wire is not constant, but depends upon the type of installation. Once installed its velocity should be reproducible; hence, some reference reflection is required for accurate fault location.

(3)   The reflection from the connector between the extension wire and the thermocouple is undetectable. The reflection due to the mismatch between extension and thermocouple wire is also small.

5.3   Tests on Installed Thermocouples

About 80 metal sheathed thermocouples of various types, sheath and insulation materials, installed in the NRU reactor were used for further TDR tests. In one group of fifteen with 50 ft fibreglas leads and 3 ft thermocouples, the welded connections between the extension wire and thermocouple were potted in epoxy and exposed to reactor conditions. About half the group had open circuited.

Comparisons of the typical reflections from a normal and a faulted thermocouple as in Figure 15 indicate the connections had open circuited. The faults are close to the junction which provides a reference reflection from a known length of thermocouple. We estimate the limits of accuracy of the indicated open circuit reflection to be within ± 1 ft of the connection. Were the fault farther from the junction, the accuracy would necessarily decrease.

Other interesting results not easily explained were noted. For example, the lossy reflection (C) in Figure 15 probably is due to insulation deterioration

THERMOCOUPLE — IRON - CON.
MgO
S.S. SHEATH
GD. JUNCTION
3' LONG, 1/8" O.D.

LEADWIRE — FIBREGLASS
No. 24 GAUGE
47' LONG

OPEN CIRCUIT

(A) REFLECTION FROM IRON LEG

(B) REFLECTION FROM CONSTANTAN LEG

OPEN CIRCUIT

NORMAL

OPEN CIRCUIT

NORMAL

20 mV

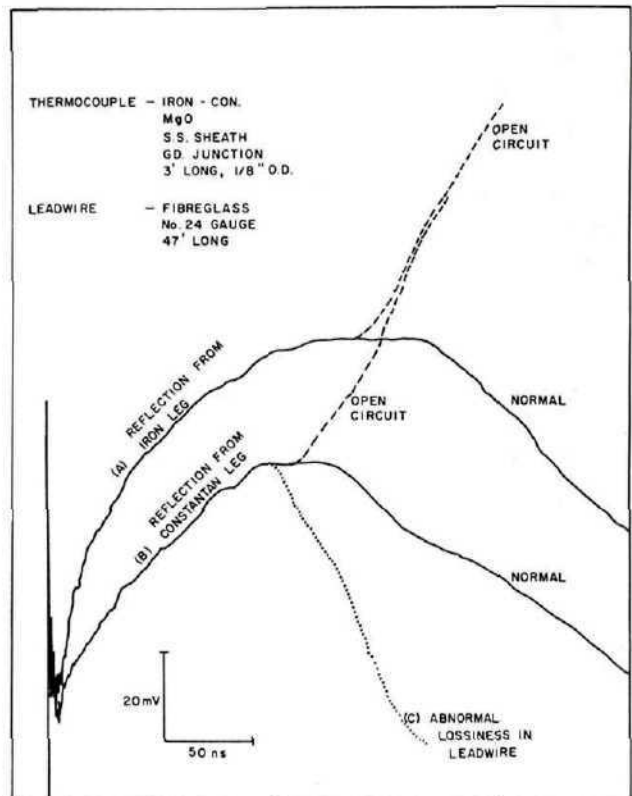50 ns

(C) ABNORMAL LOSSINESS IN LEADWIRE

Figure   15.   Comparison between Sound and Faulty Thermocouples Installed in Reactor

or other material changes of radiated fibreglas, since this reflection is similar to a short or low resistance condition which agrees with a decrease in loop resistance. In one thermocouple of the same group, the iron leg had faulted at the potted connection but the constantan wire remained unbroken.

Other groups of thermocouples were 15 ft long with 35 ft of extension wire, and the connection made outside the reactor. Comparisons of the reflections from various groups identical except for their sheath material (stainless steel or aluminum) or their insulation (alumina or magnesia) did not reveal differences which could be attributed to either of these variations. Also, the reflections from these groups were unchanged by the reactor's operating temperature.

The small reflection due to the impedance mismatch at the connection between extension wire and thermocouple which was noted in Figure 13 was observed in some of the other thermocouple groups. Because of this random behaviour and its small amplitude, this reflection cannot be depended upon to indicate the connection point.

6. CONCLUSIONS AND RECOMMENDATIONS

1. Lossy reflections can not be mathematically defined except in one simple case. A basic understanding of transmission line principles is more helpful in interpreting the acutal reflections.

2. Pulse attenuation due to series resistance of the thermocouple and the variations of pulse velocity along unshielded extension wire are the chief difficulties in TDR applications to thermocouples.

3. Accurate fault location for unshielded extension wire is possible only when comparisons with other sound thermocouples of identical construction, length and installation can be made. Alternately, a "calibration" reflection should be recorded just after installation to establish the pulse velocity and initial impedance profile for later comparisons.

4. Faults within a few feet of the junction in a thermocouple 50 ft long have been located with accuracies of ± 1ft. We estimate that faults in thermocouples up to 25 ft long with up to 75 ft of lead wire may usually be located within 10% of the actual location if a trace previous to faulting is available for comparison. This knowledge of the fault location should be a definite aid to replacement and repair procedures, particularly for inaccessable thermocouples.

5. This technique could be used to investigate failures in other in-pile instrumentation such as flux detectors or resistance bulbs.

7. ACKNOWLEDGEMENT

8. BIBLIOGRAPHY

1. B. M. Oliver - "Time Domain Reflectometry", Hewlett-Packard Journal, Vol. 15, No. 6, February 1964. Other publications also.

2. Hewlett-Packard Application Note 62.

3. J. L. Stewart - "Circuit Anaylsis of Transmission Lines", Wiley, 1958.

4. F. E. Nixon - "Handbook of Laplace Transformation", Prentice Hall, 1960.

5. H. A. Wheeler - "Transmission Line Impedance Curves", Proc. IRE, Vol. 38, Page 1400, December 1950.

6. H. B. Dwight - "Tables of Integrals and other Mathematical Data", MacMillan Company, 1961.

APPENDIX A

Method of Determining the Series Resistance

A lossy transmission line may be approximated as a series resistor and capacitor.

From (1) if $G = 0$

$$Z_L = \left[\frac{L}{C}\right]^{1/2} \left[1 + \frac{R}{sL}\right]^{1/2}$$

If $x < 1$, $(1+x)^a \cong 1 + ax$, and if $R << sL$,

then Z_L can be approximated as

$$Z_L = \left[\frac{L}{C}\right]^{1/2}\left[1 + \frac{R}{2sL}\right] = R' + \frac{1}{sC'}$$

where $R' = \left[\frac{L}{C}\right]^{1/2}$ and $C' = \frac{2\sqrt{LC}}{R}$

Thus a lossy line acts as a resistor in series with a capacitor if these approximations are valid. This is similar to the circuit of Figure 4. The reflection from such a circuit is derived in the theory and is there given by equation (7).

$$e^-(t) = E\left[1 - \frac{2Z_0}{R' + Z_0} \exp \frac{-t}{(R' + Z_0)C'}\right]$$

The slope at $t = 0$ is $\frac{de^-(t)}{dt}\Big]_{t=0} = \frac{2EZ_0}{(R' + Z_0)^2 C}$

where Z_0 is the impedance of the generator.

APPENDIX B

Reflection from an Infinite Lossy Line

For a lossy thermocouple the series resistive losses cannot be ignored. The following analysis is from Hewlett-Packard Journal, Vol. 15, February 1964.

The line impedance is defined as;

$$Z_L = \left[\frac{R + sL}{G + sC}\right]^{1/2} = Z_0 \left[\frac{s + \eta}{s + \sigma}\right]^{1/2} \quad (1B)$$

where $\eta = \frac{R}{L}$

and $\sigma = \dfrac{G}{C}$

$$Z_o = \left[\dfrac{L}{C}\right]^{1/2}$$

If this line terminates a loss free line or a generator of characteristic impedance Z_o, the reflection coefficient is;

$$k_r = \dfrac{e^-}{e^+} \dfrac{Z_o - Z_L}{Z_o + Z_L} = \dfrac{\sqrt{s+\eta} - \sqrt{s+\sigma}}{\sqrt{s+\eta} + \sqrt{s+\sigma}} \qquad (2B)$$

If a unit impulse is applied to the line, then the Fourier transform of the expression for k_r defines the reflection as a function of time.

$$f'(t) = \dfrac{1}{t} I_1\left[\dfrac{\eta - \sigma}{2} \cdot t\right] \exp \dfrac{\eta + \sigma}{2} \cdot t \qquad (3B)$$

If G is negligible, $\sigma = 0$.

The response to a step function input is the integral of f'(t) so that for a unit step function the reflection is

$$f(t) = 1 - \left\{ I_o\left[\dfrac{\eta\,t}{2}\right] + I_1\left[\dfrac{\eta\,t}{2}\right] \exp \dfrac{-\eta\,t}{2} \right\} \quad (4B)$$

where $I_o\left[\dfrac{\eta\,t}{2}\right]$ and $I_1\left[\dfrac{\eta\,t}{2}\right]$ are modified Bessel functions of the first and second kind respectively.

The slope of this curve at t = 0 is given by the limit of Equation 3B as t approaches zero.

$$\left. f'(t) \right]_{t \to o} = \dfrac{\eta - \sigma}{4} \qquad (5B)$$

HEWLETT **hp** PACKARD